CALET: Calorimetric Electron Telescope

DSU Conference
Annecy, 2018 June 27

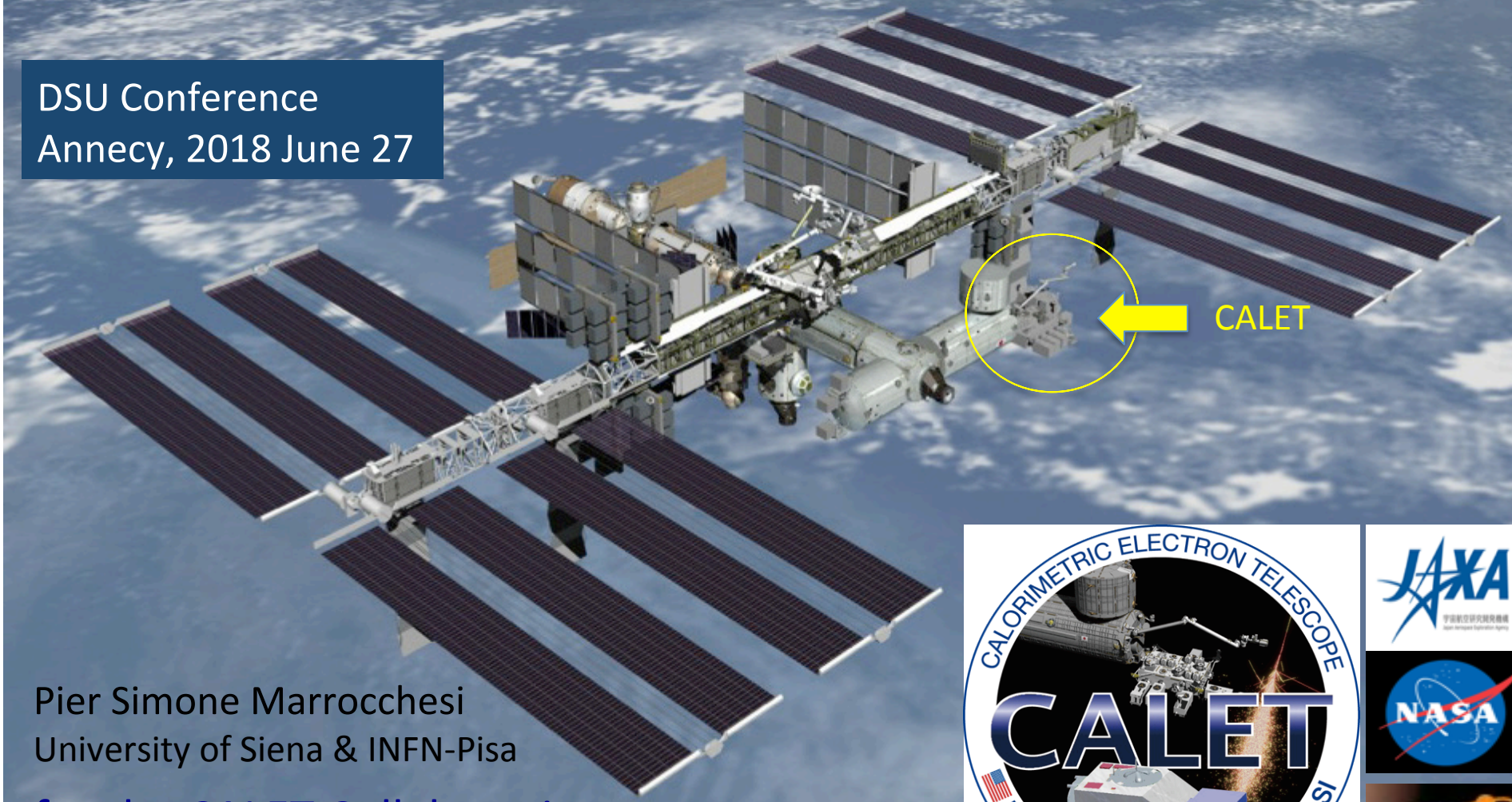

Pier Simone Marrocchesi
University of Siena & INFN-Pisa

for the CALET Collaboration

CALET collaboration team

O. Adriani[25], Y. Akaike[2], K. Asano[7], Y. Asaoka[9,31], M.G. Bagliesi[29], G. Bigongiari[29], W.R. Binns[32], S. Bonechi[29], M. Bongi[25], P. Brogi[29], J.H. Buckley[32], N. Cannady[12], G. Castellini[25], C. Checchia[26], M.L. Cherry[12], G. Collazuol[26], V. Di Felice[28], K. Ebisawa[8], H. Fuke[8], G.A. de Nalfo [14], T.G. Guzik[12], T. Hams[3], M. Hareyama[23], N. Hasebe[31], K. Hibino[10], M. Ichimura[4], K. Ioka[34], W.Ishizaki[7], M.H. Israel[32], A. Javaid[12], K. Kasahara[31], J. Kataoka[31], R. Kataoka[16], Y. Katayose[33], C. Kato[22], Y.Kawakubo[1], N. Kawanaka[30], H. Kitamura[15], H.S. Krawczynski[32], J.F. Krizmanic[2], S. Kuramata[4], T. Lomtadze[27], P. Maestro[29], P.S. Marrocchesi[29], A.M. Messineo[27], J.W. Mitchell[14], S. Miyake[5], K. Mizutani[20], A.A. Moiseev[3], K. Mori[9,31], M. Mori[19], N. Mori[25], H.M. Motz[31], K. Munakata[22], H. Murakami[31], Y.E. Nakagawa[8], S. Nakahira[9], J. Nishimura[8], S. Okuno[10], J.F. Ormes[24], S. Ozawa[31], L. Pacini[25], F. Palma[28], P. Papini[25], A.V. Penacchioni[29], B.F. Rauch[32], S.B. Ricciarini[25], K. Sakai[3], T. Sakamoto[1], M. Sasaki[3], Y. Shimizu[10], A. Shiomi[17], R. Sparvoli[28], P. Spillantini[25], F. Stolzi[29], I. Takahashi[11], M. Takayanagi[8], M. Takita[7], T. Tamura[10], N. Tateyama[10], T. Terasawa[7], H. Tomida[8], S. Torii[9,31], Y. Tunesada[18], Y. Uchihori[15], S. Ueno[8], E. Vannuccini[25], J.P. Wefel[12], K. Yamaoka[13], S. Yanagita[6], A. Yoshida[1], K. Yoshida[21], and T. Yuda[7]

1) Aoyama Gakuin University, Japan
2) CRESST/NASA/GSFC and Universities Space Research Association, USA
3) CRESST/NASA/GSFC and University of Maryland, USA
4) Hirosaki University, Japan
5) Ibaraki National College of Technology, Japan
6) Ibaraki University, Japan
7) ICRR, University of Tokyo, Japan
8) ISAS/JAXA Japan
9) JAXA, Japan
10) Kanagawa University, Japan
11) Kavli IPMU, University of Tokyo, Japan
12) Louisiana State University, USA
13) Nagoya University, Japan
14) NASA/GSFC, USA
15) National Inst. of Radiological Sciences, Japan
16) National Institute of Polar Research, Japan
17) Nihon University, Japan
18) Osaka City University, Japan
19) Ritsumeikan University, Japan
20) Saitama University, Japan
21) Shibaura Institute of Technology, Japan
22) Shinshu University, Japan
23) St. Marianna University School of Medicine, Japan
24) University of Denver, USA
25) University of Florence, IFAC (CNR) and INFN, Italy
26) University of Padova and INFN, Italy
27) University of Pisa and INFN, Italy
28) University of Rome Tor Vergata and INFN, Italy
29) University of Siena and INFN, Italy
30) University of Tokyo, Japan
31) Waseda University, Japan
32) Washington University-St. Louis, USA
33) Yokohama National University, Japan
34) Yukawa Institute for Theoretical Physics, Kyoto University, Japan

CALET collaboration team

O. Adriani[25], Y. Akaike[2], K. Asano[7], Y. Asaoka[9,31], M.G. Bagliesi[29], G. Bigongiari[29], W.R. Binns[32], S. Bonechi[29], M. Bongi[25], P. Brogi[29], J.H. Buckley[32], N. Cannady[12], G. Castellini[25], C. Checchia[26], M.L. Cherry[12], G. Collazuol[26], V. Di Felice[28], K. Ebisawa[8], H. Fuke[8], G.A. de Nalfo [14], T.G. Guzik[12], T. Hams[3], M. Hareyama[23], N. Hasebe[31], K. Hibino[10], M. Ichimura[4], K. Ioka[34], W.Ishizaki[7], M.H. Israel[32], A. Javaid[12], K. Kasahara[31], J. Kataoka[31], R. Kataoka[16], Y. Katayose[33], C. Kato[22], Y.Kawakubo[1], N. Kawanaka[30], H. Kitamura[15], H.S. Krawczynski[32], J.F. Krizmanic[2], S. Kuramata[4], T. Lomtadze[27], P. Maestro[29], P.S. Marrocchesi[29], A.M. Messineo[27], J.W. Mitchell[14], S. Miyake[5], K. Mizutani[20], A.A. Moiseev[3], K. Mori[9,31], M. Mori[19], N. Mori[25], H.M. Motz[31], K. Munakata[22], H. Murakami[31], Y.E. Nakagawa[8], S. Nakahira[9], J. Nishimura[8], S. Okuno[10], J.F. Ormes[24], S. Ozawa[31], L. Pacini[25], F. Palma[28], P. Papini[25], A.V. Penacchioni[29], B.F. Rauch[32], S.B. Ricciarini[25], K. Sakai[3], T. Sakamoto[1], M. Sasaki[3], Y. Shimizu[10], A. Shiomi[17], R. Sparvoli[28], P. Spillantini[25], F. Stolzi[29], I. Takahashi[11], M. Takayanagi[8], M. Takita[7], T. Tamura[10], N. Tateyama[10], T. Terasawa[7], H. Tomida[8], S. Torii[9,31], Y. Tunesada[18], Y. Uchihori[15], S. Ueno[8], E. Vannuccini[25], J.P. Wefel[12], K. Yamaoka[13], S. Yanagita[6], A. Yoshida[1], K. Yoshida[21], and T. Yuda[7]

CALET Payload

Kounotori (HTV) 5

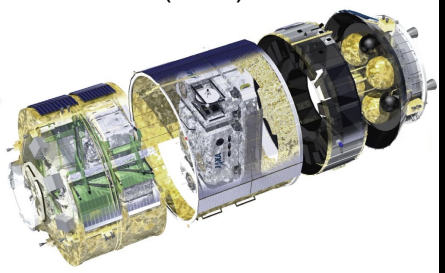

Launched on Aug. 19th, 2015
by the Japanese H2-B rocket

Emplaced on JEM-EF port #9
on Aug. 25th, 2015
(JEM-EF: Japanese Experiment Module-Exposed Facility)

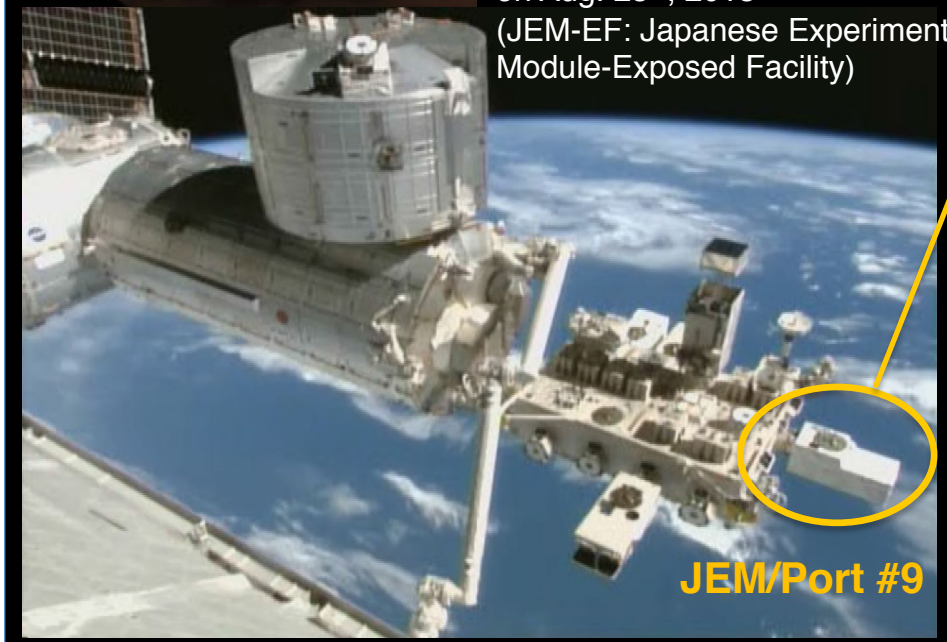

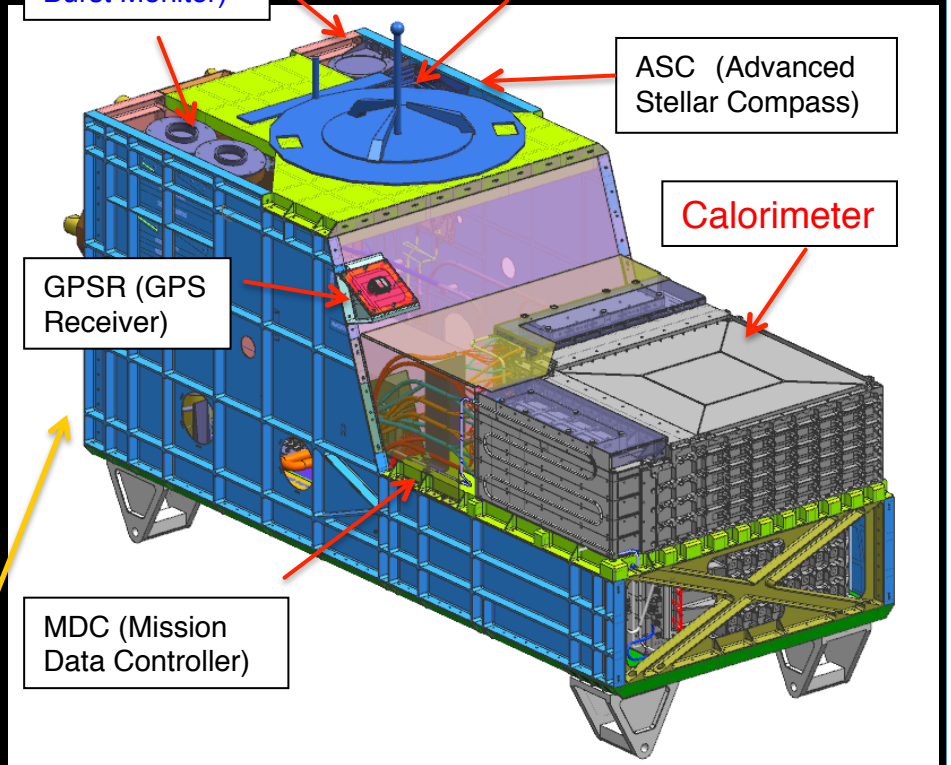

- Mass: 612.8 kg
- JEM Standard Payload Size:
  1850mm (L) × 800mm (W) × 1000mm (H)
- Power Consumption: 507 W (max)
- Telemetry:
  Medium 600 kbps (6.5GB/day) / Low 50 kbps

ISS: a Cosmic Ray Observatory in Low Earth Orbit

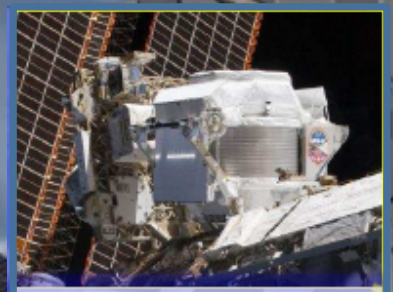

AMS Launch
May 16, 2011

ISS-CREAM Launch
August 14, 2017

CALET Launch
August 19, 2015

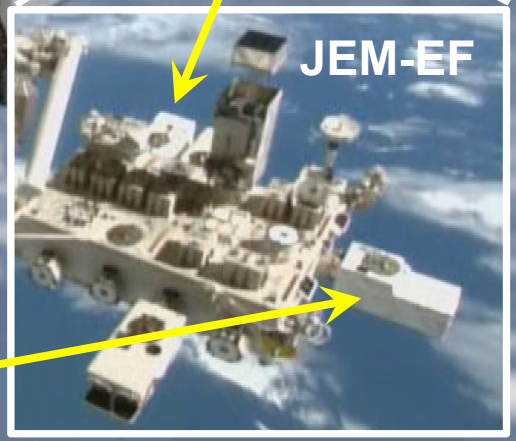

CALET Capability

Field of view: ~ 45 degrees (from the zenith)

Geometrical Factor: ~ 1,040 cm^{2}sr (for electrons)

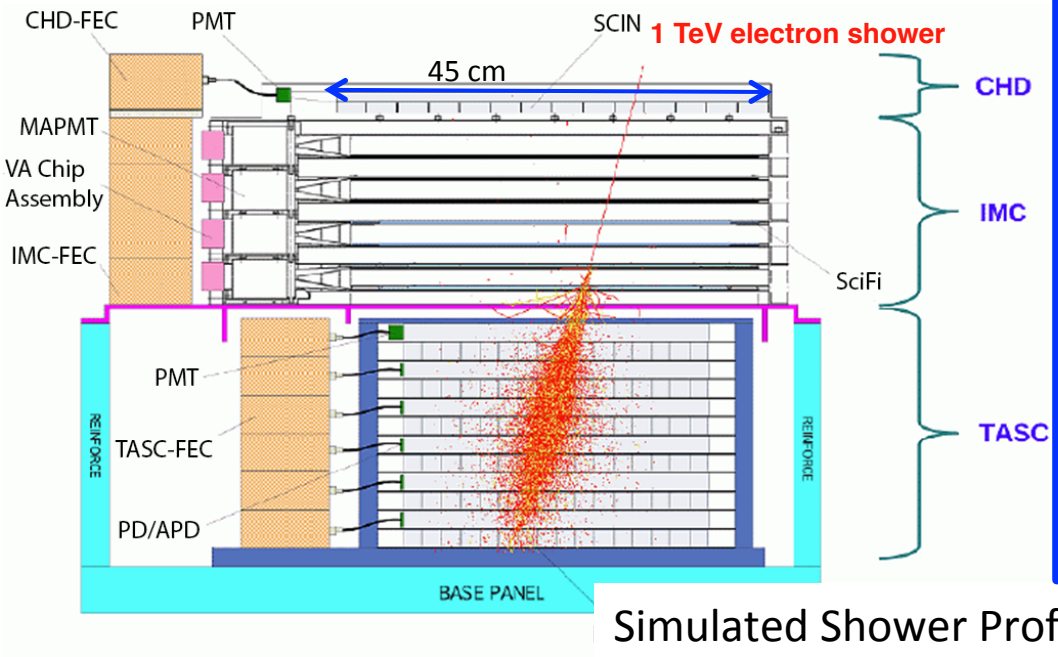

CALET: a unique set of key instruments

- **CHD**: a dedicated charge detector + multiple dE/dx sampling in the IMC allow to **identify individual nuclear species** (Δz~0.15-0.3 e).
- **IMC**: a high granularity (1mm) imaging pre-shower calorimeter accurately identifies **the arrival direction** of incident particles (~0.1°) and the **starting point** of electro-magnetic showers.
- **TASC**: a thick (~30 X_0), fully active calorimeter allows to extend electron measurements into the TeV energy region with ~2% **energy resolution**.
- Combined, they **separate electrons** from the abundant protons (rejection > 10^5).

Simulated Shower Profile

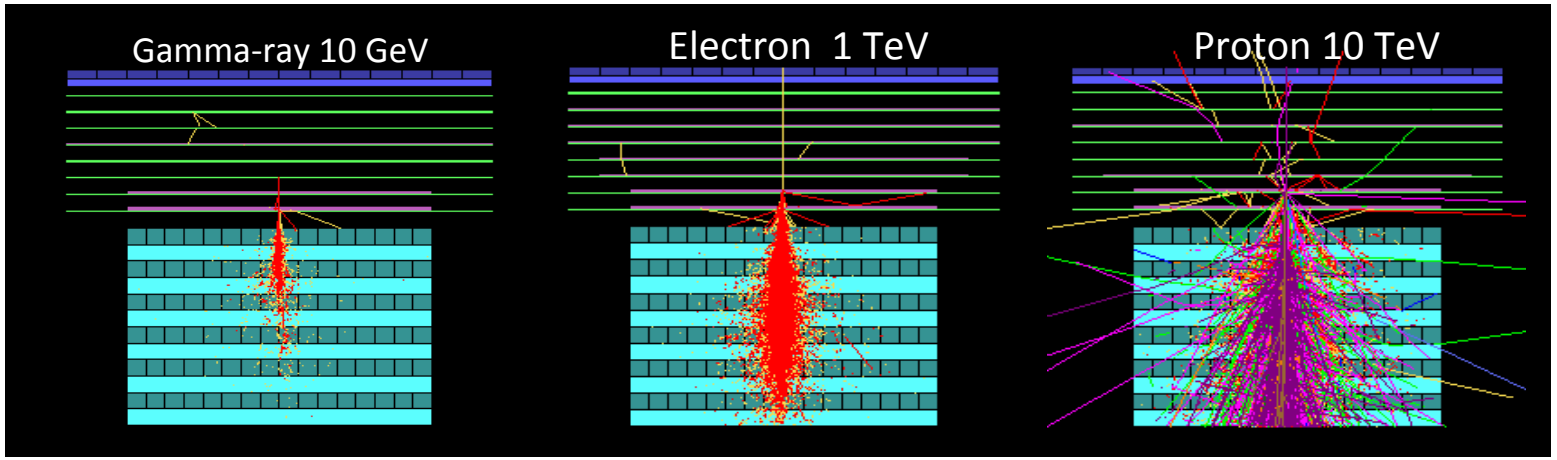

CALET Instrument

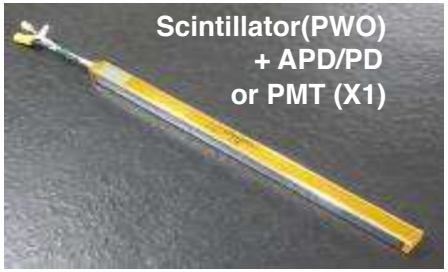

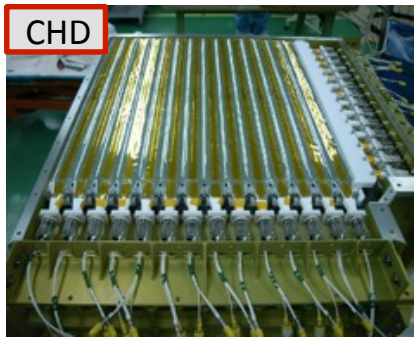

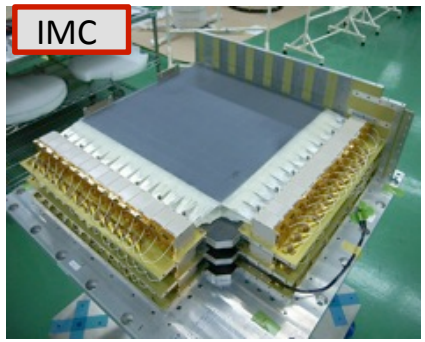

CALORIMETER

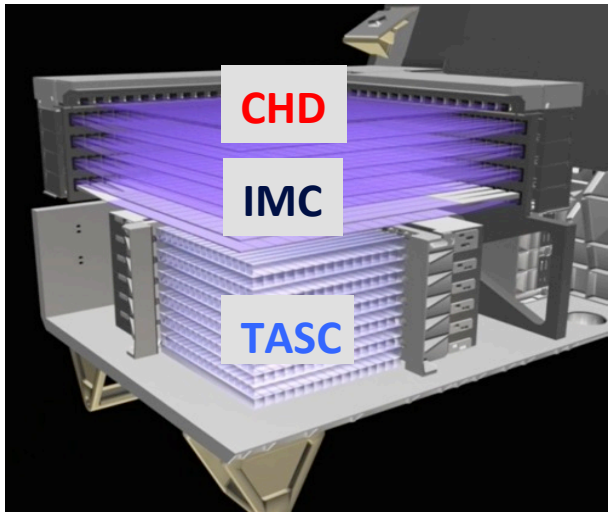

	CHD (Charge Detector)	IMC (Imaging Calorimeter)	TASC (Total Absorption Calorimeter)
Measure	**Charge (Z=1-40)**	**Tracking , Particle ID**	**Energy, e/p Separation**
Geometry (Material)	**Plastic Scintillators**: 28 paddles 14 paddles x 2 layers (X,Y) Paddle Size: 32 x 10 x 450 mm^3	**Scintillating Fibers**: 448 x 16 layers (X,Y) 7 W layers ($3X_0$): $0.2X_0$ x 5 + $1X_0$ x2 Scifi size: 1 x 1 x 448 mm^3	**PWO logs**: 16 x 12 layers (x,y): 192 logs log size: 19 x 20 x 326 mm^3 Total Thickness: 27 X_0 , ~1.2 λ_I
Readout	**PMT+CSA**	**64-anode PMT+ ASIC**	**APD/PD+CSA** **PMT+CSA (for Trigger)@top layer**

✧ CALET **tracking** takes advantage of the IMAGING capabilities of IMC thanks to its granularity of 1 mm with Sci-fibers **readout individually**.

Example: A multi-prong event due to an interaction of the primary particle in the CHD is very well imaged by the IMC.

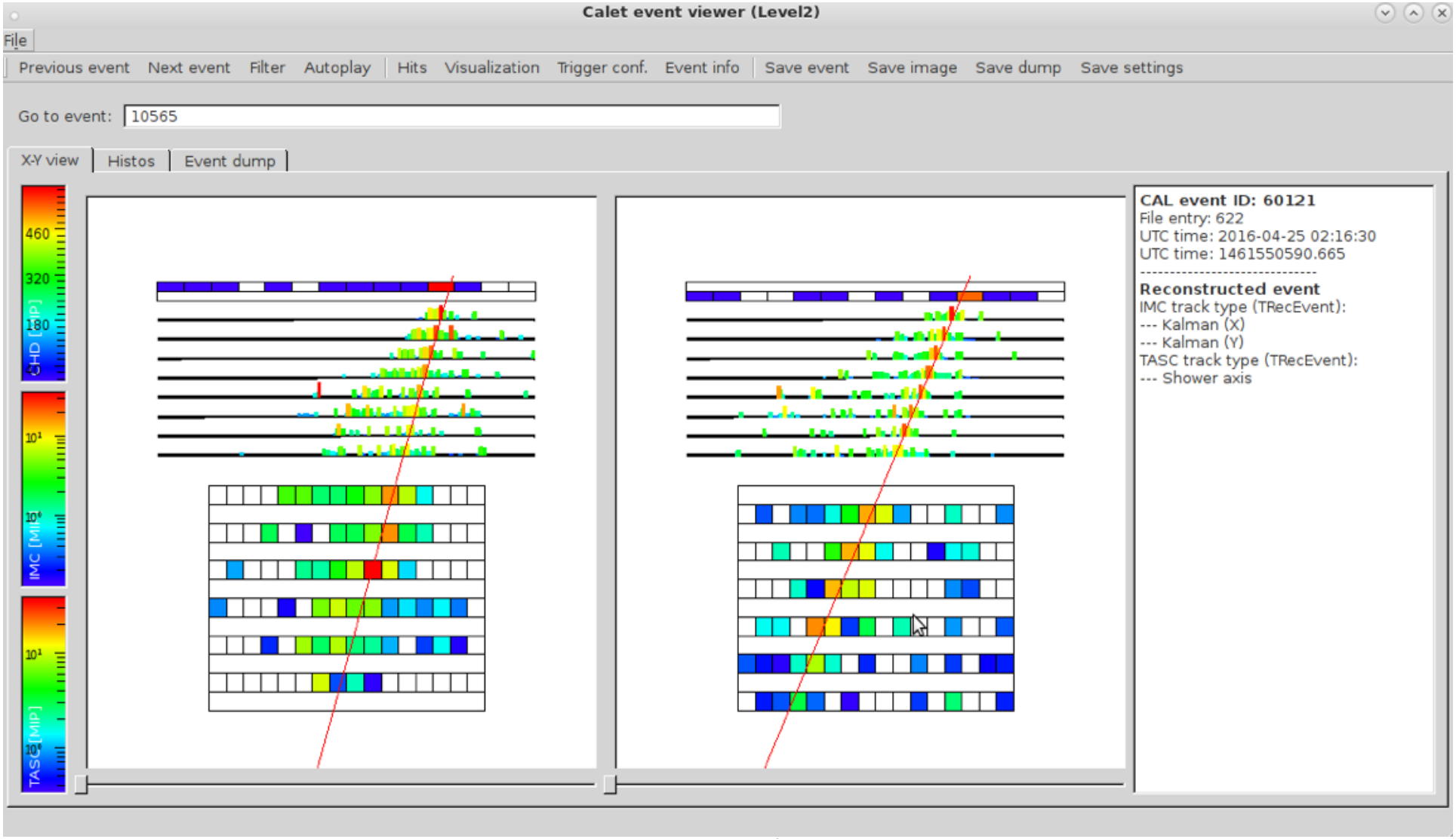

TASC Energy Measurement: wide Dynamical Range 1-10^6 MIPs

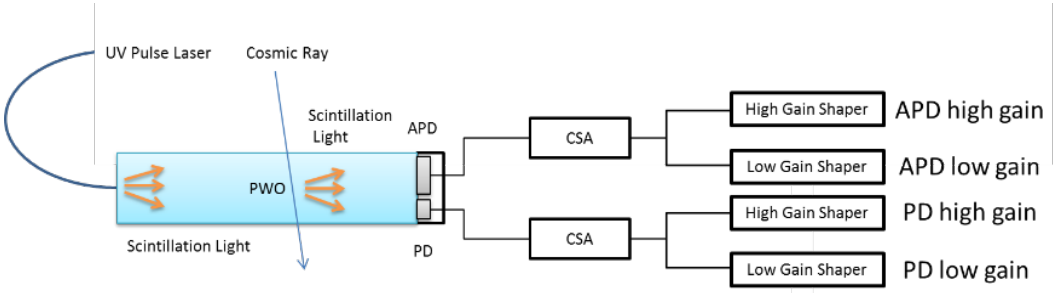

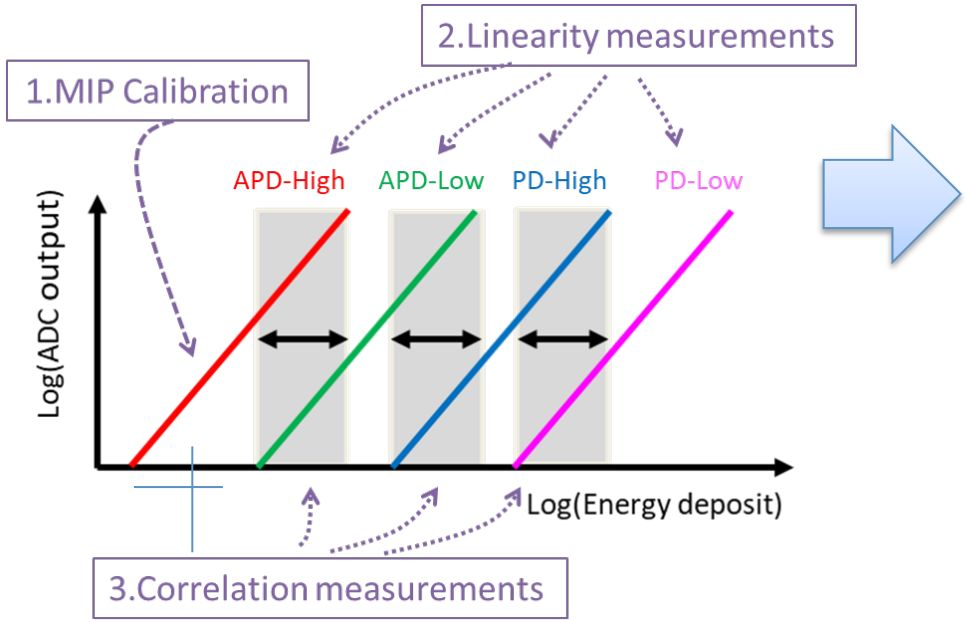

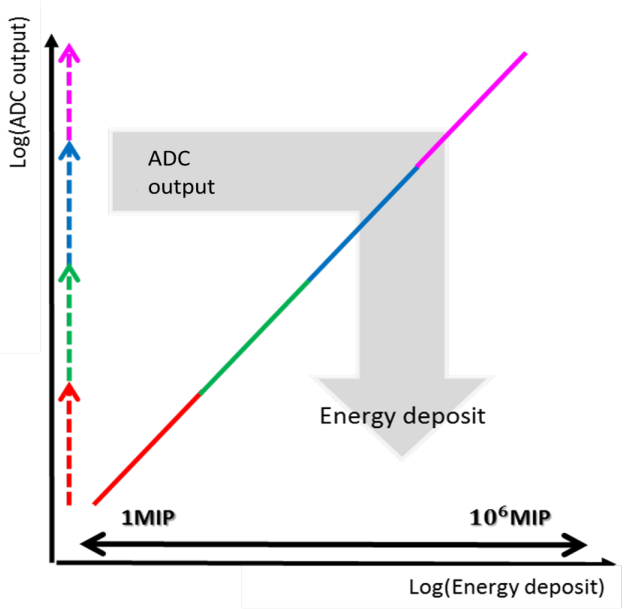

Example of energy measurement in one log of TASC

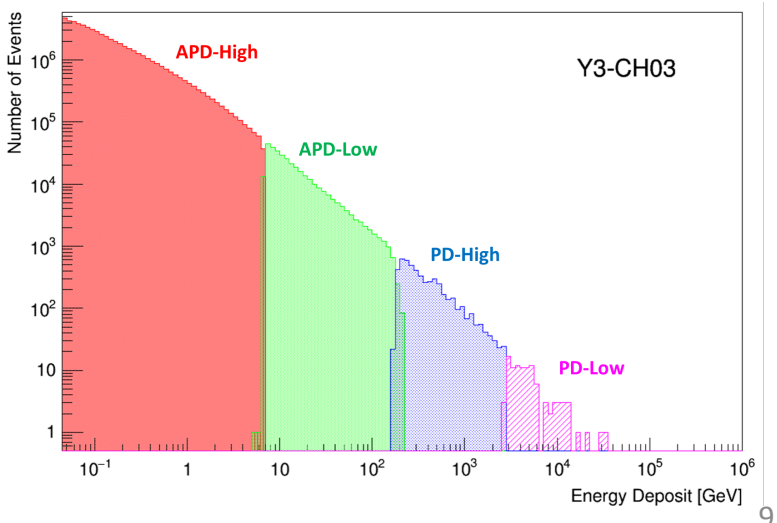

Details of our energy calibration can be found at:
Y.Asaoka, Y.Akaike, Y.Komiya, R.Miyata, S.Torii et al., Astropart. Phys. 91 (2017) 1.

Main Scientific Objectives

Scientific Objectives	Observation Targets	Energy Range
CR Origin and Acceleration	Electron spectrum p→Fe individual spectra Ultra Heavy Ions ($26 < Z \leq 40$) Gamma-rays (Diffuse + Point sources)	1GeV - 20 TeV 10 GeV - 1000 TeV > 600 MeV/n 1 GeV - 1 TeV
Galactic CR Propagation	B/C and sub-Fe/Fe ratios	Up to some TeV/n
Nearby CR Sources	Electron spectrum	100 GeV - 20 TeV
Dark Matter	Signatures in electron/gamma-ray spectra	100 GeV - 20 TeV
Solar Physics	Electron flux (1GeV-10GeV)	< 10 GeV
Gamma-ray Transients	Gamma-rays and X-rays	7 keV - 20 MeV

- Electron observation in 1 GeV - 20 TeV is achieved with high energy resolution due to design optimization for electron detection Search for Dark Matter and Nearby Sources
- Observation of cosmic-ray nuclei will be performed in energy region from 10 GeV to 1 PeV
  Unravelling the CR acceleration and propagation mechanism(s)
- Detection of transient phenomena in space by stable observations
  Gamma-ray bursts, Solar flares, e.m. counterpart from GW sources, ...

CALET Main Target: Identification of Electron Sources

Some nearby sources, e.g. Vela SNR, are likely to have unique signatures in the electron energy spectrum at the TeV scale (Kobayashi et al. ApJ 2004)

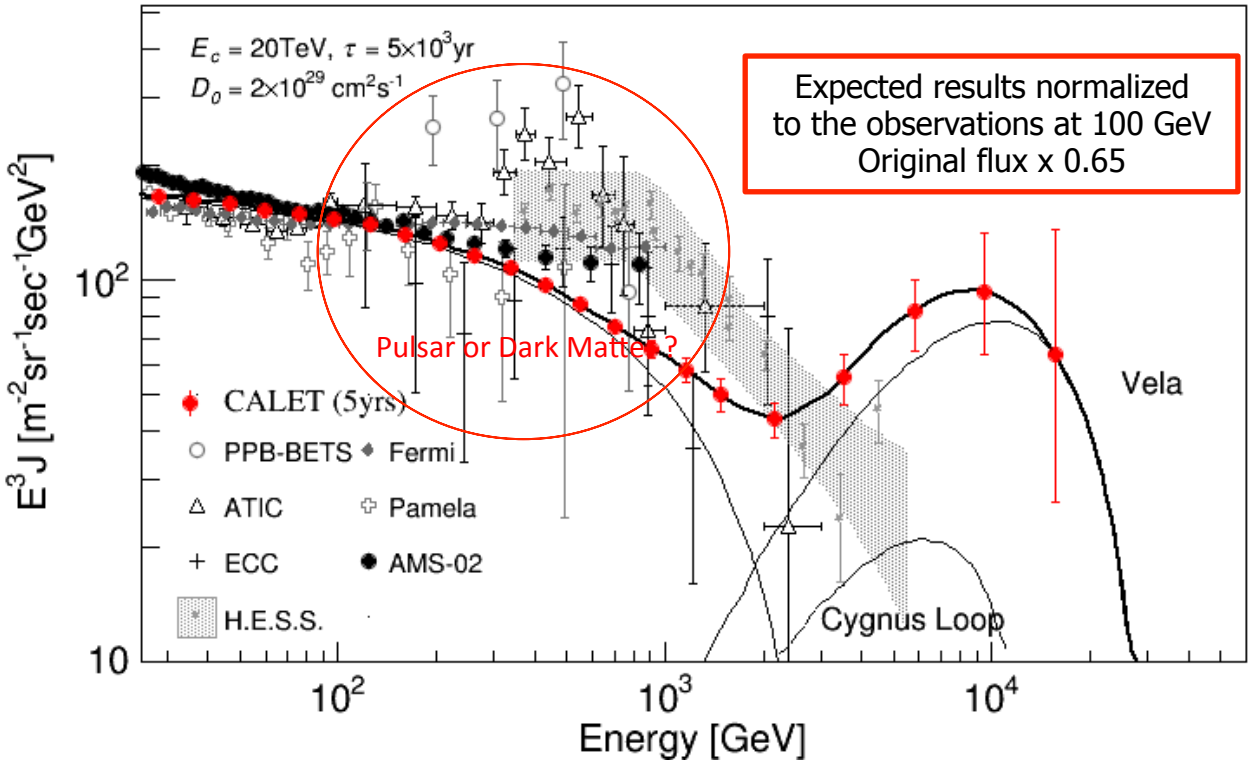

Expected Anisotropy from Vela

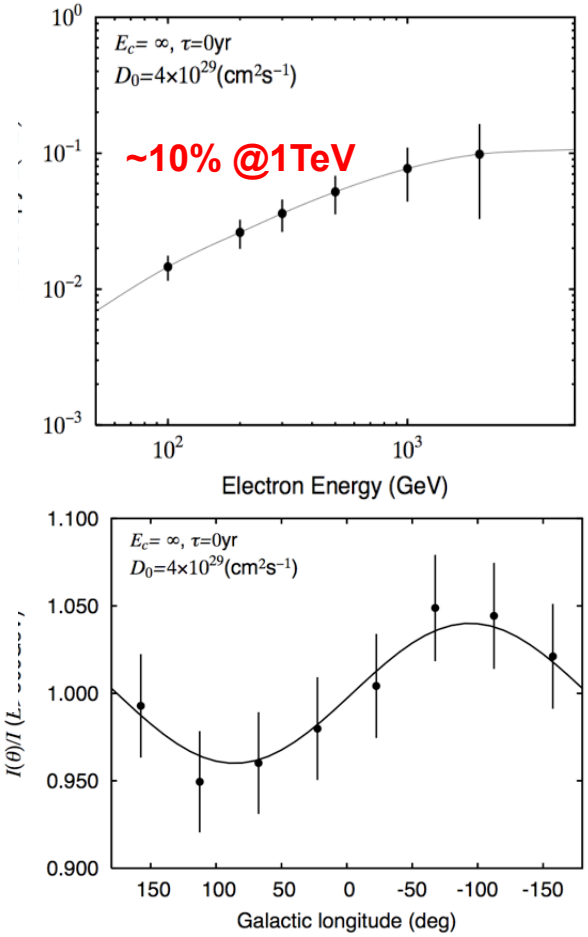

possible identification of the unique signature from nearby SRNs, such as Vela, in the electron spectrum by CALET in the TeV region

CALET: Cosmic-Ray Nuclei Spectra in the Multi-TeV region

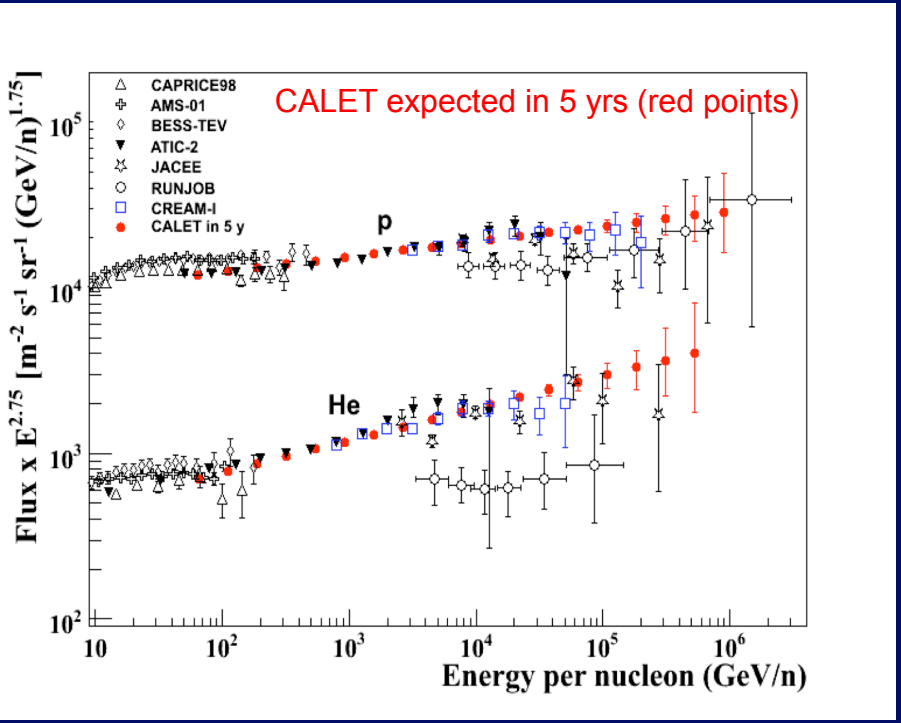

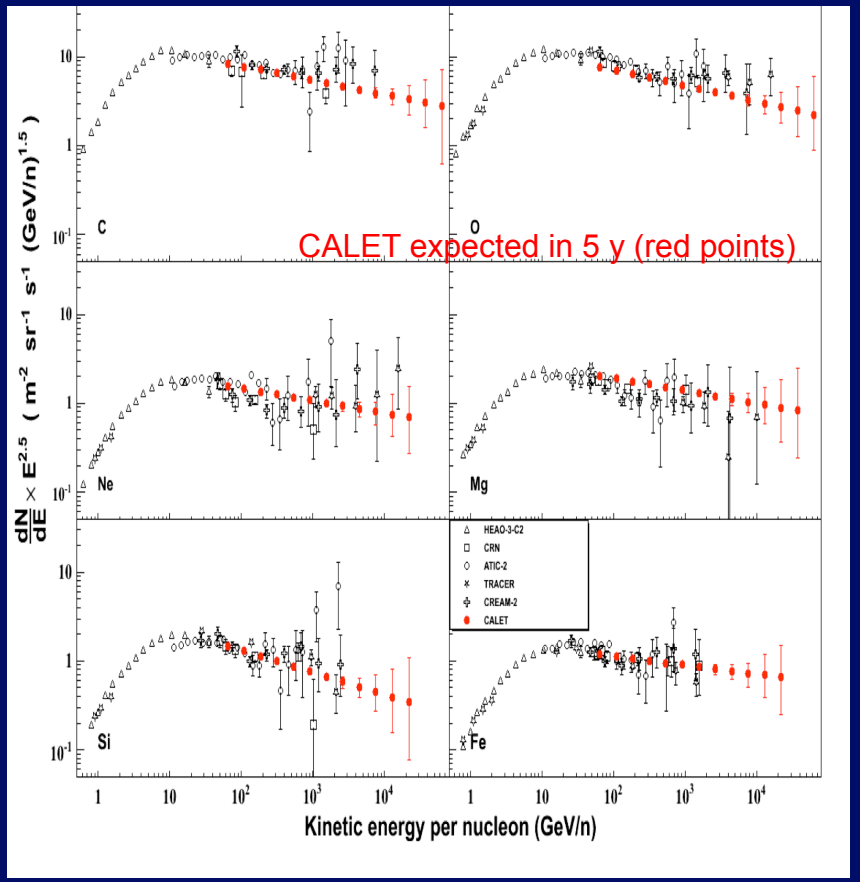

- Proton spectrum to ≈ 900 TeV
- He spectrum to ≈ 400 TeV/n
- Spectra of C,O,Ne,Mg,Si to ≈ 20 TeV/n
- B/C ratio to ≈ 4 - 6 TeV/n
- Fe spectrum to ≈ 10 TeV/n

CALET energy reach
(5 years)

Observation by High Energy Trigger (>10GeV)

Observation by High Energy Trigger for 870 days : Oct.13, 2015 – Dec.31, 2017

- The exposure, SΩT, has reached to ~76.0 m^2 sr day for electron observations by continuous and stable operations.
- Total number of the triggered events is ~ 570 million with a live time fraction of 85.0 %.

Accumulated observation time (live, dead)

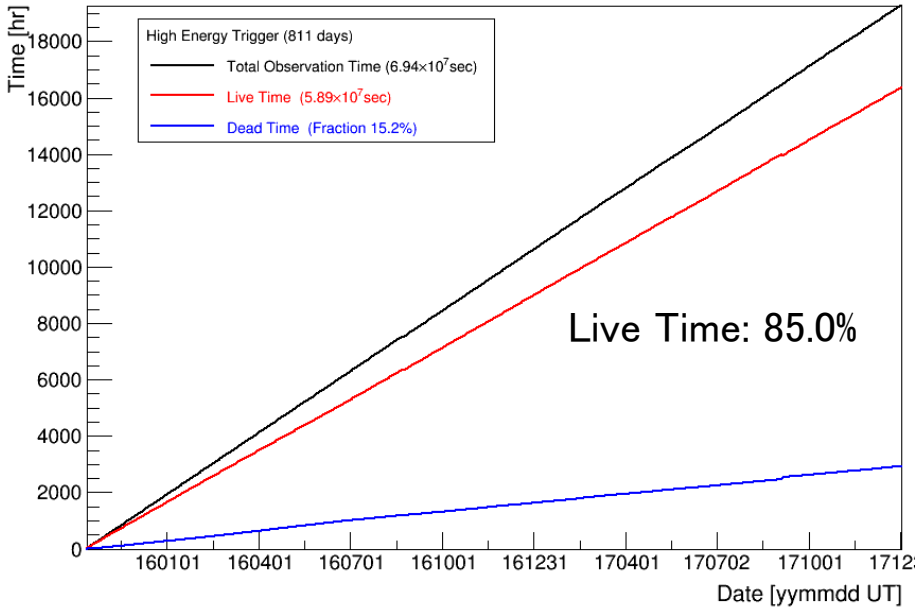

Accumulated triggered event number

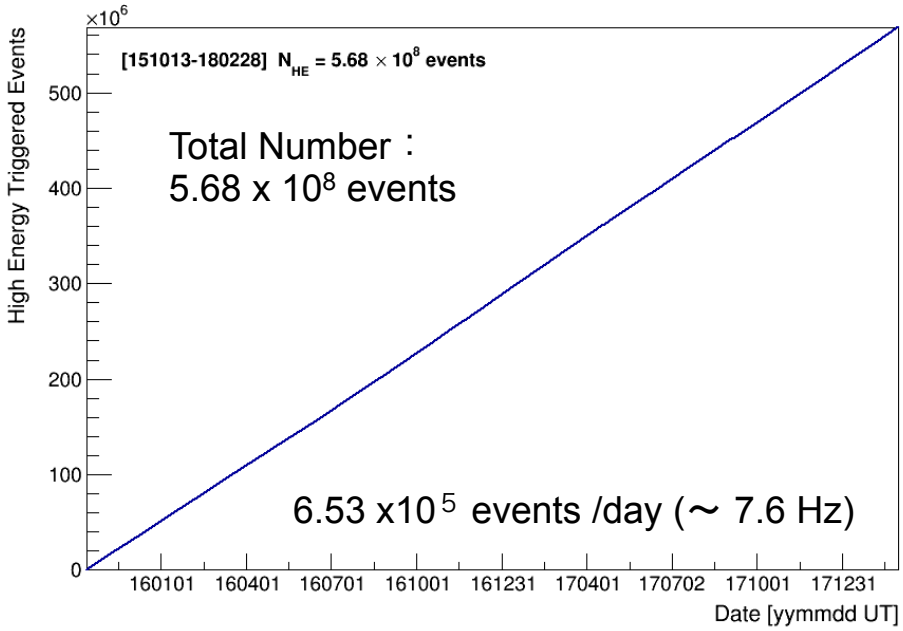

Examples of Observed Events

Event Display: Electron Candidate (>100 GeV)

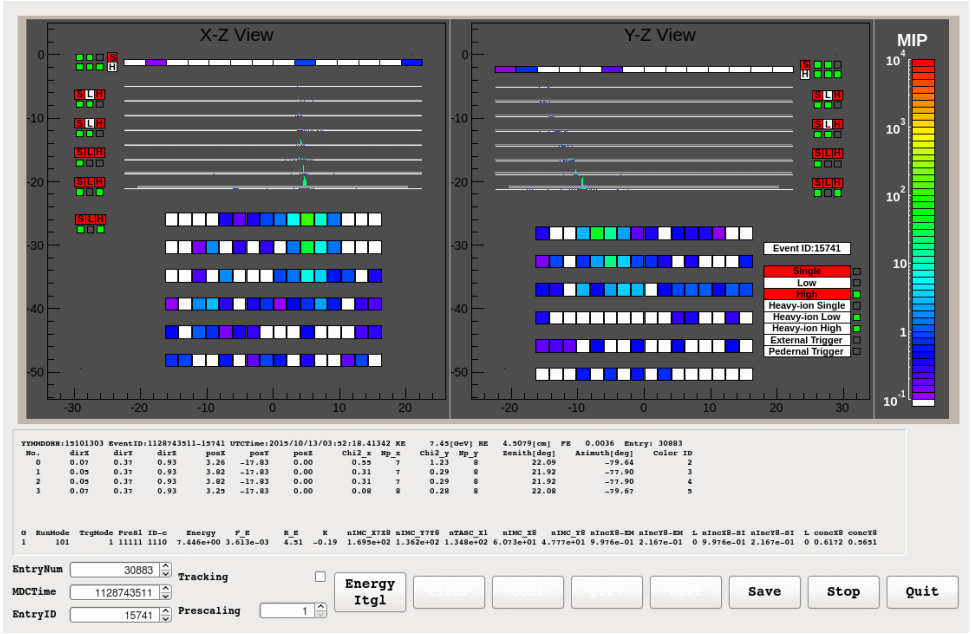

Proton, ΔE=2.89 TeV

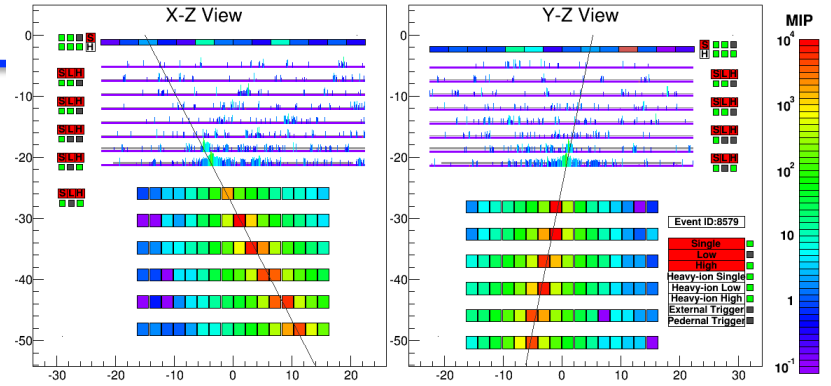

Fe, ΔE=9.3 TeV

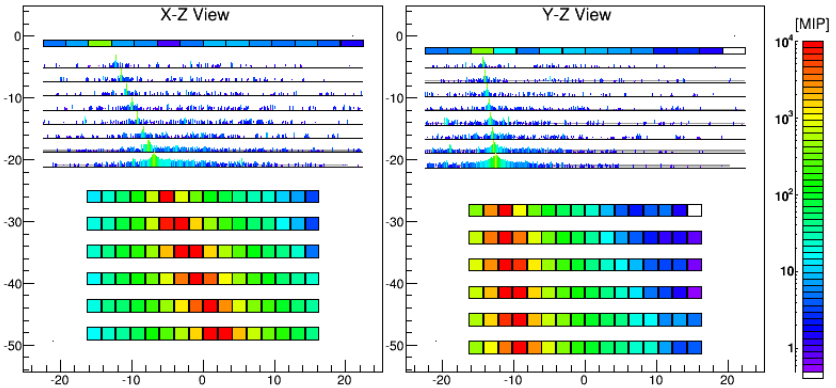

Electron, E=3.05 TeV

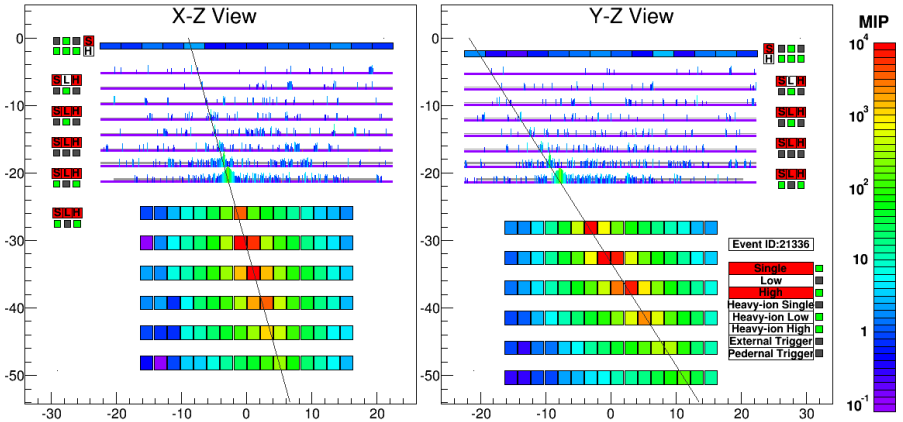

Gamma-ray, E=44.3 GeV

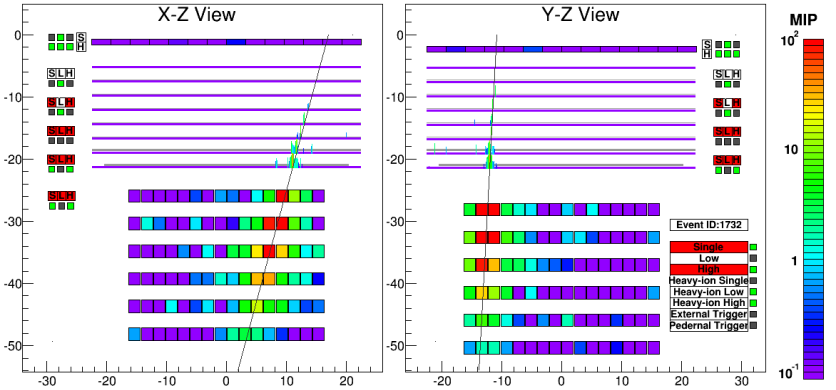

ISS Radiation Environment

South Atlantic Anomaly (SAA)

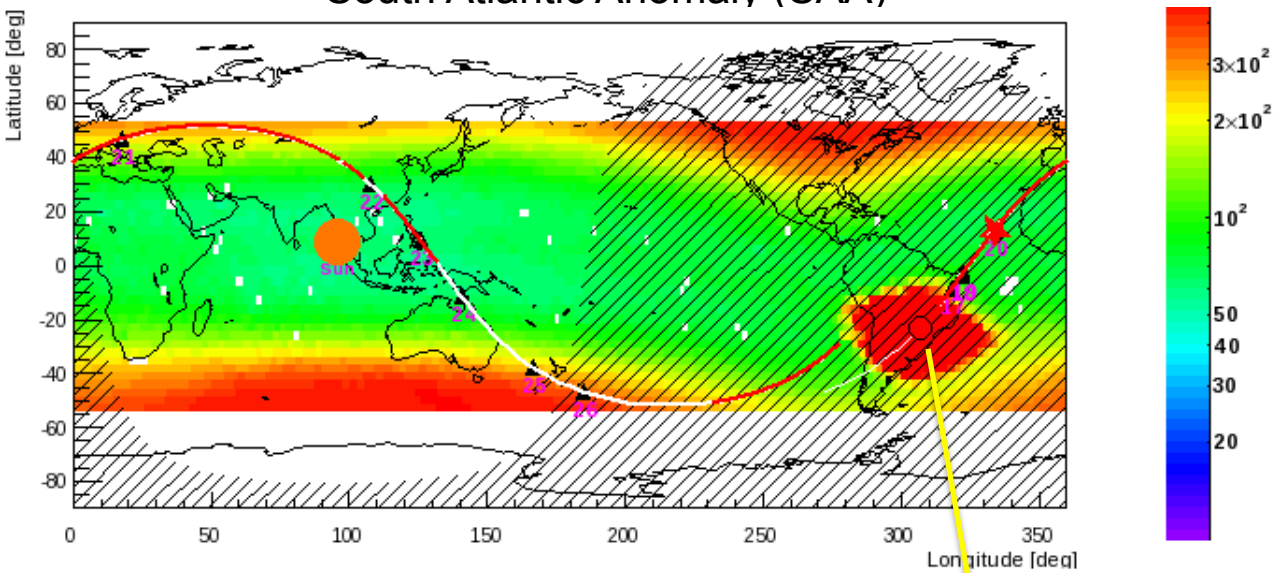

ISS orbit
@ 2017/08/29 5:25UT
ISS ran through SAA.

CHD count rate jumped up to ~3×10^5 Hz from 10^3 Hz, but the HE trigger rate remained stable.

Trigger/Count Rate
@ 2017/08/29

HE trigger was not affected by SAA thanks to high energy threshold (>10 GeV).
(Energies of the trapped particles are too low to make a trigger for the observations.)

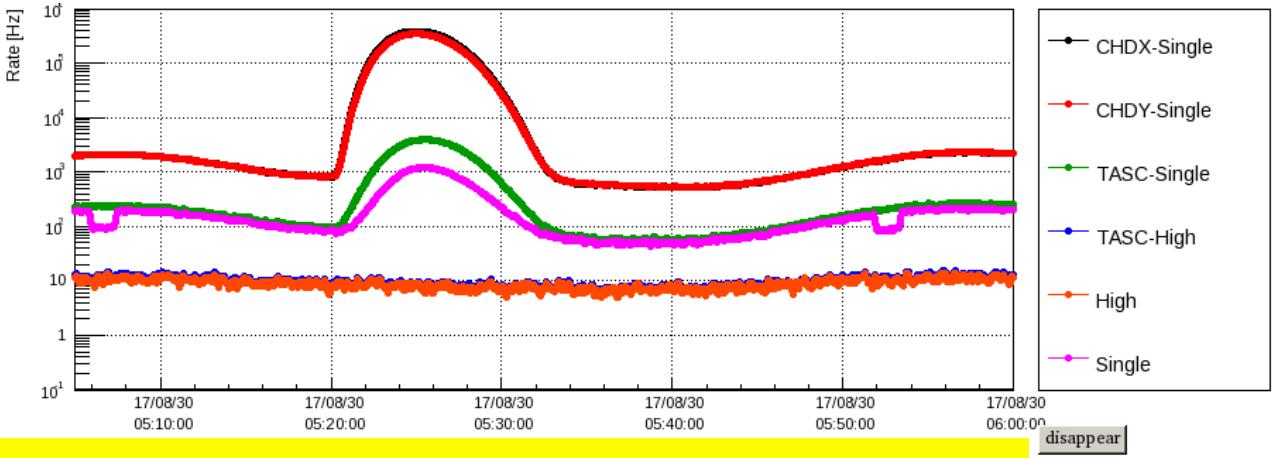

⇒ Observation is continuously carried out even at SAA!

Position and Temperature Calibration, and Long-term Stability

Example of position dependence correction

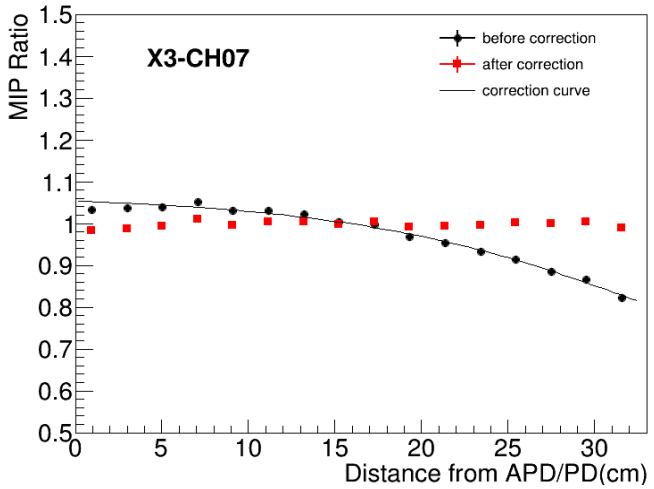

Examples of temperature change correction

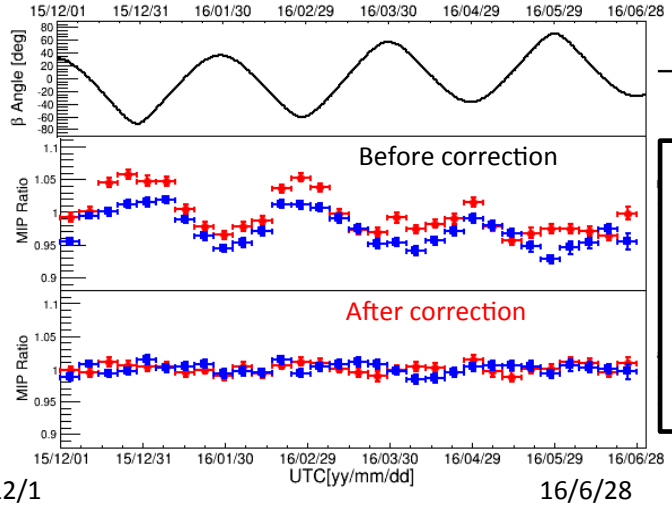

TASC

Active Thermal Control System (ATCS) on ISS can provide very stable thermal condition during Long-tem observations: Δt ~ a few degrees

Example of long-term variation correction

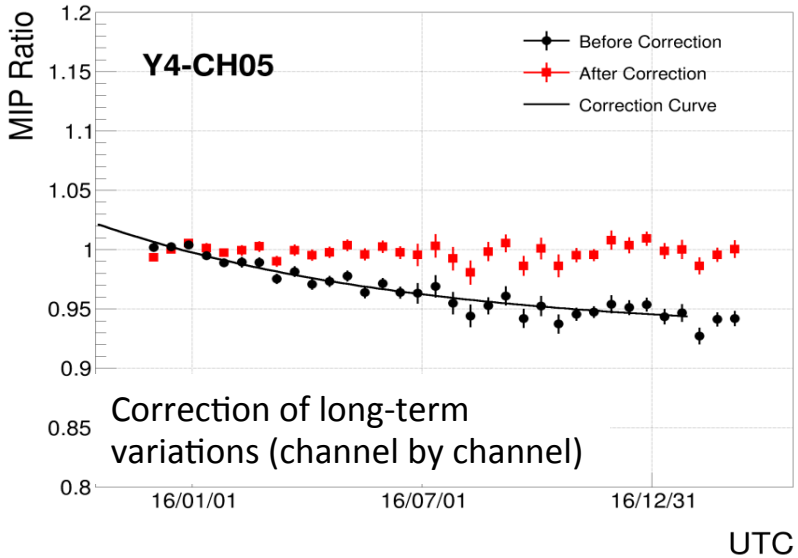

Distribution of MIPs for 192 ch x 16 segmented positions after each correction

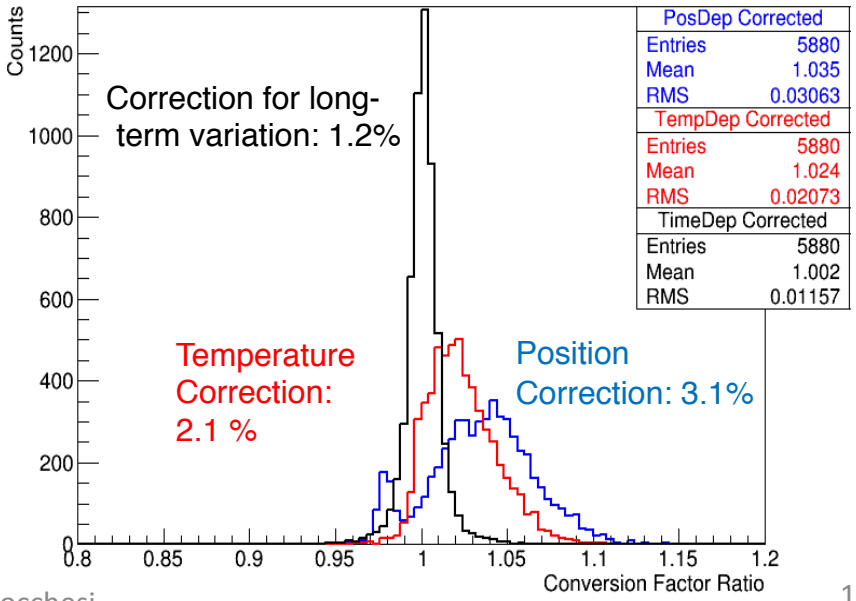

Energy Resolution for Electrons by On-orbit Calibration

Y.Asaoka, Y.Akaike, Y.Komiya, R.Miyata, S.Torii et al., Astroparticle Physics 91 (2017) 1.

Considering the calibration errors and instrument noise, energy resolution is estimated as a function of energy.

Energy dependence of energy resolution

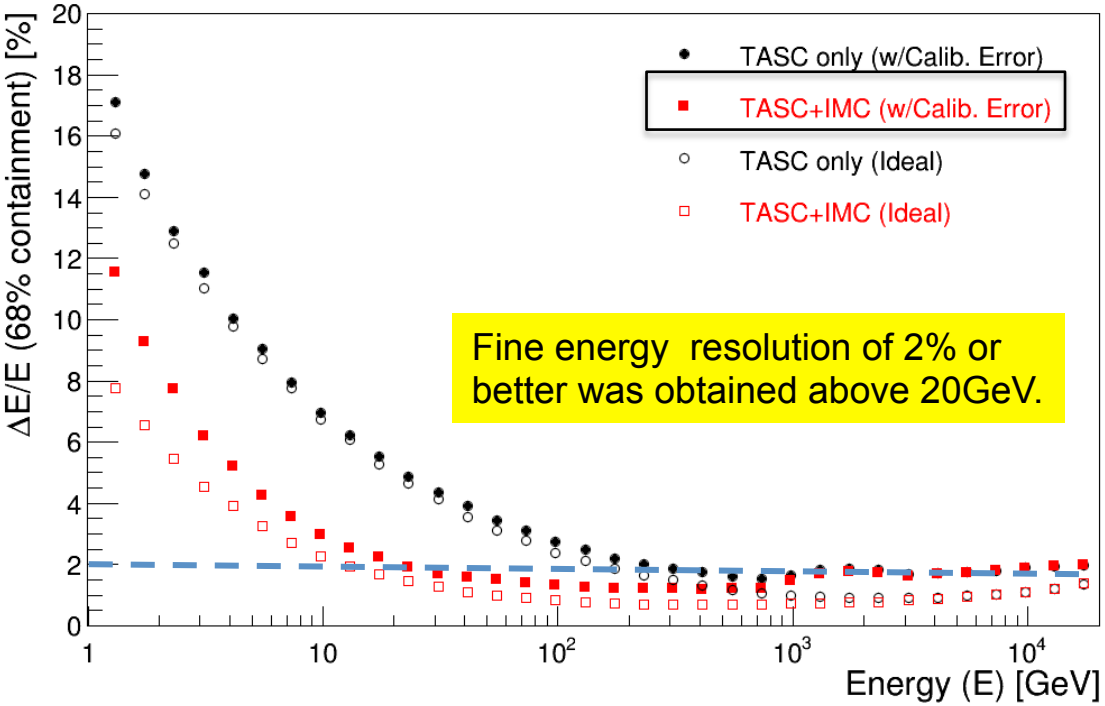

Error budget in energy calibration

MIP	Energy conversion	2.6%
	Peak fitting of MC and flight data	0.6%
	Fitting range dependence	0.6%(*)
	Position dependence	1.8%
	Temperature dependence	1.0%
	Rigidity cutoff dependence	1.0%(*)
	Systematic uncertainty estimated from p/He consistency	1.0%
UV Laser	Linearity	1.4~2.5%
	Fit error	
	APD high gain	1.4%
	APD low gain	1.5%
	PD high gain	2.5%
	PD low gain	2.2%
Gain Ratio	Gain range connection	1.6~2.1%
	Fit error	
	APD-high to APD-low gain	0.1%
	APD-low to PD-high gain	0.7%
	PD high to PD low gain	0.1%
	Slope extrapolation	
	APD-high to APD-low gain	1.6%
	APD-low to PD-high gain	2.0%(*)
	PD high to PD low gain	1.8%
Sampling Bias		0.5%(**)

(*) also considered as systematic error on energy scale
(**) energy-scale systematic error only

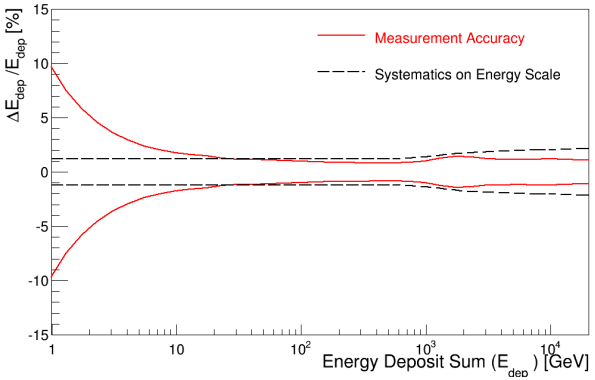

Electron Analysis: Characteristics of TeV Electron and Proton Showers

Simple and high-efficiency electron identification is possible even at TeV.

⇒ CALET is best suited for observation of possible narrow structures in the total electron spectrum in the trans-TeV region.

Flight Data (detector size in cm)

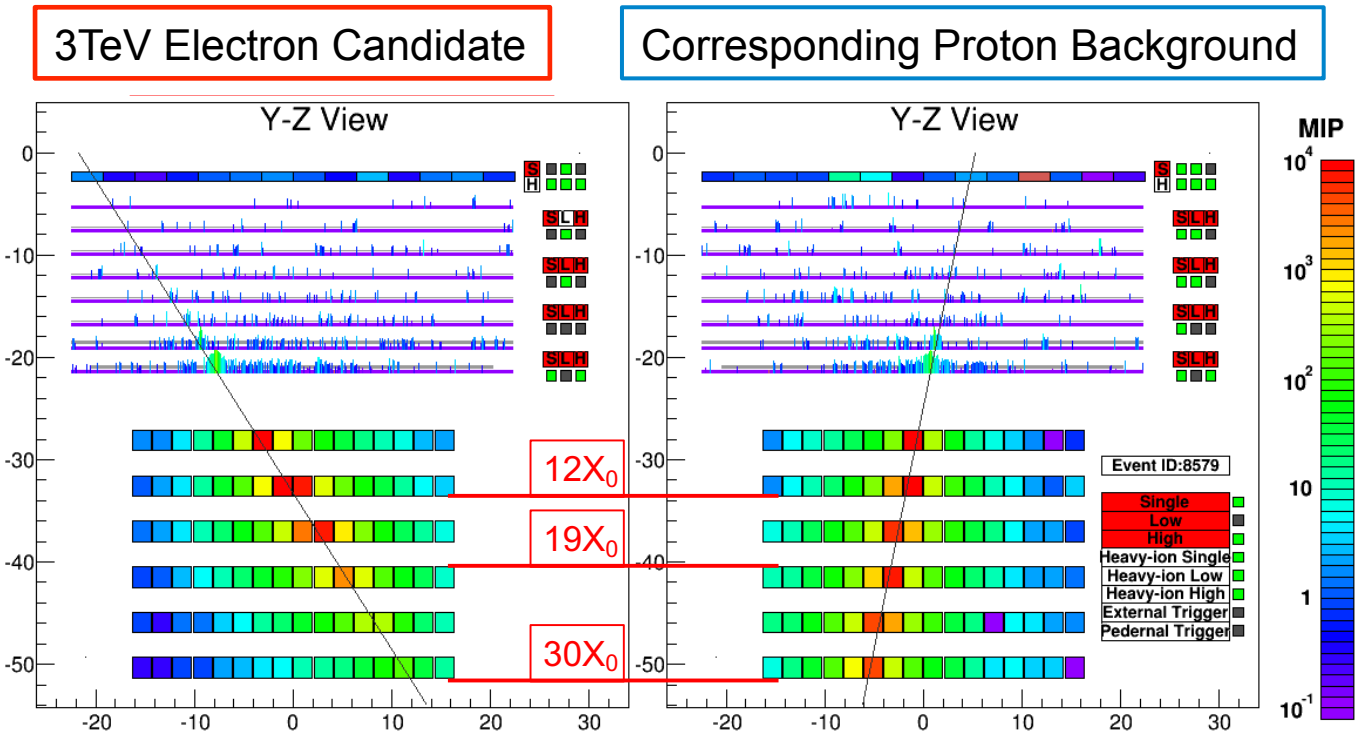

Electron / Proton Separation

Simple Two Parameter Cut

F_E: Energy fraction of the bottom layer sum to the whole energy deposit sum in TASC

R_E: Lateral spread of energy deposit in TASC-X1

Cut Parameter K is defined as follows:

$K = \log_{10}(F_E) + 0.5\ R_E$ (/cm)

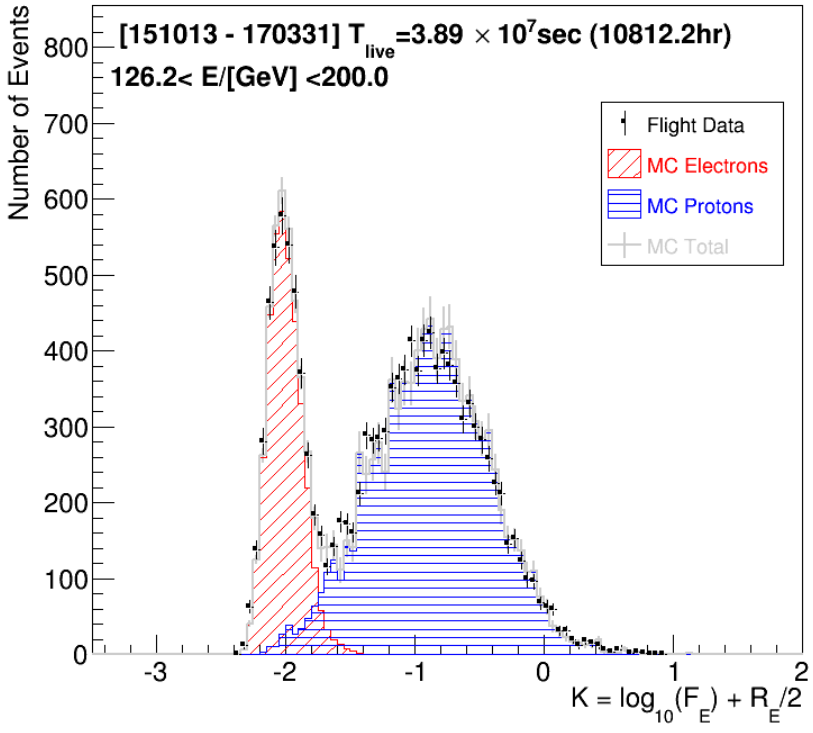

Boosted Decision Trees (BDT)

In addition to the two parameters in the left, TASC and IMC shower profile fits are used as discriminating variables

BDT Response using 9 parameters

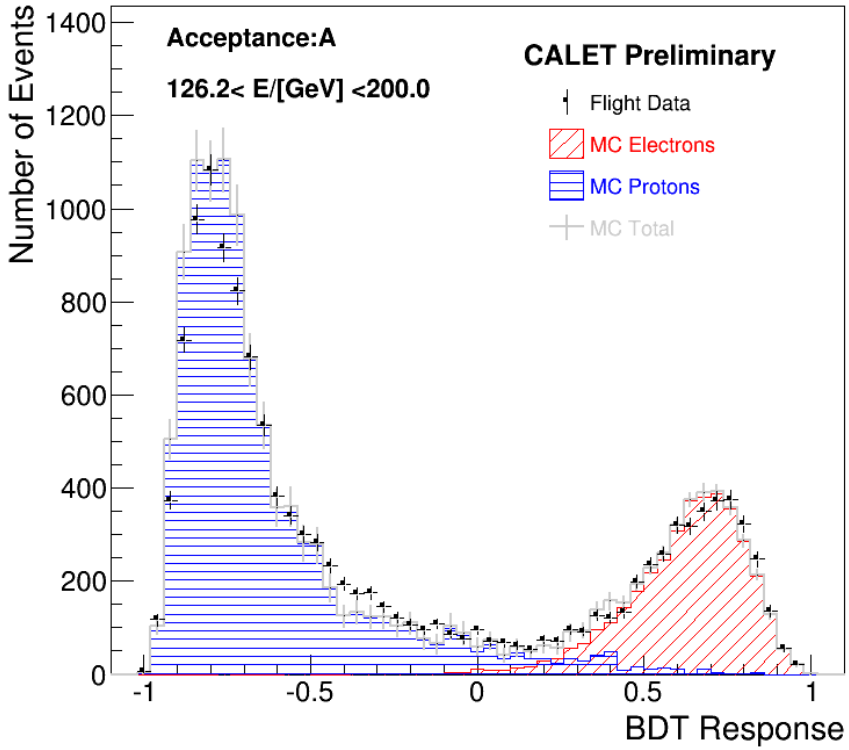

e/p Discrimination Power by Analysis of BDT and K parameter

Distribution of BDT Response

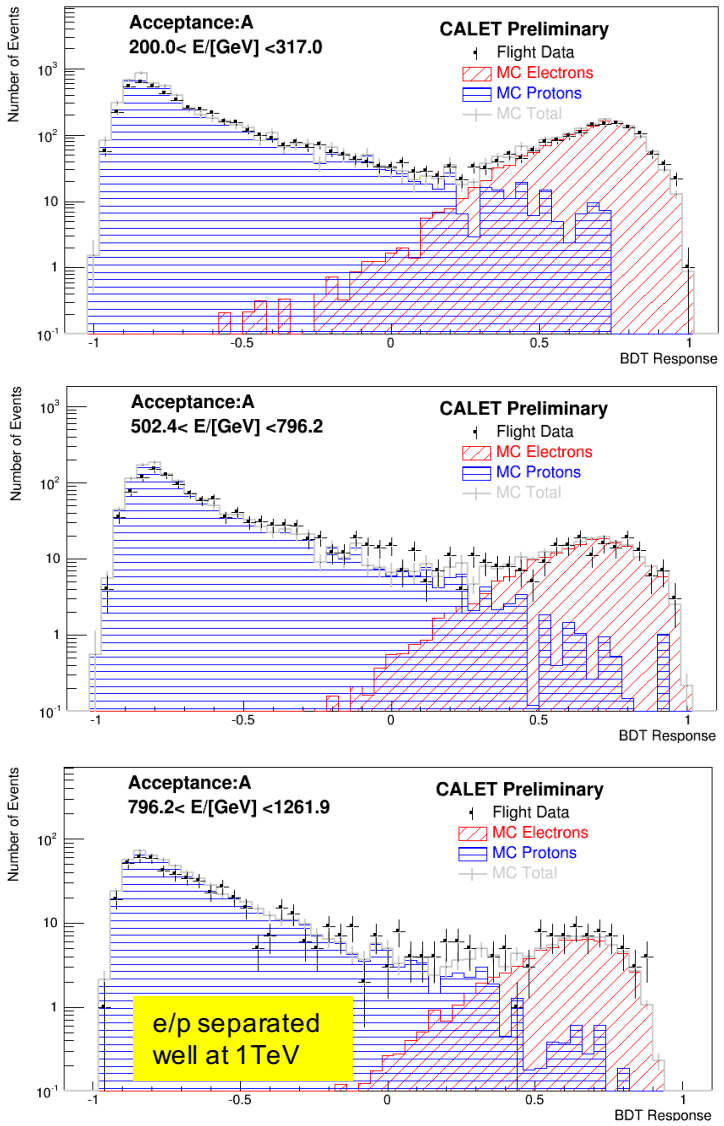

Electron Efficiency

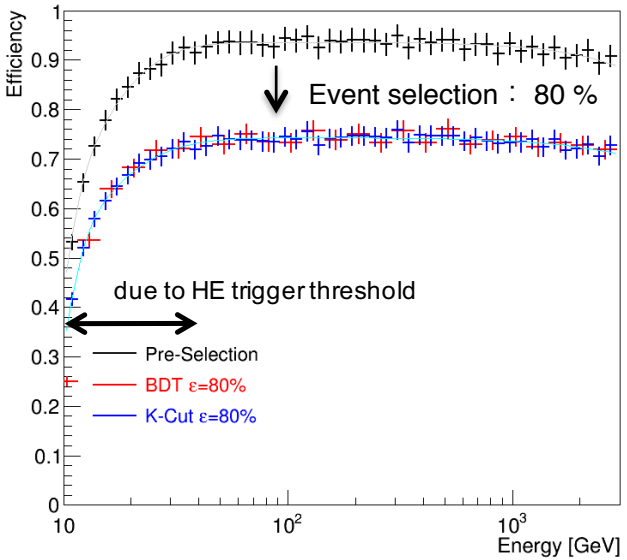

Proton contamination Ratio

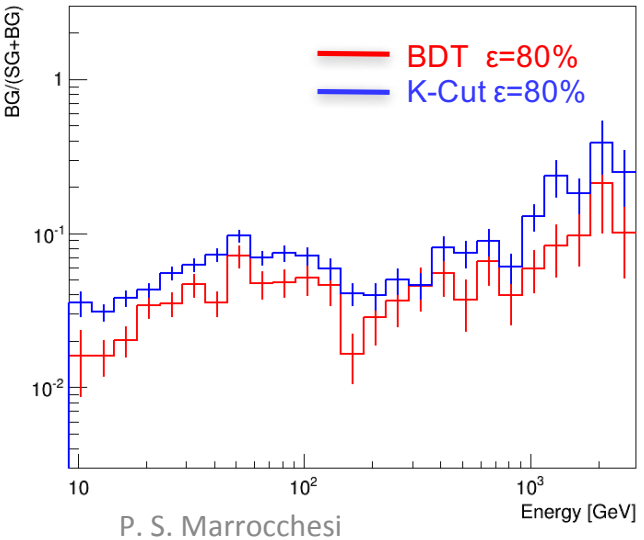

- KEY POINT: high and almost energy independent efficiency
- The efficiencies of K-cut and BDT have very similar energy dependence.
- Electron efficiency after pre-selection and e/p separation is considerably high (~70%) and ~constant above HE trigger threshold.
- Simple two parameter cut is used in the lower energy region (< 500GeV), while the difference in resultant spectrum are taken into account in the systematic uncertainty.
- proton contamination is 2 - 5 % in 10 GeV-1 TeV, 5-10 % above 1 TeV with BDT analysis. (improving with analysis)

Systematic Uncertainties in Derivation of Energy Spectrum

Stability of resultant flux are intensively studied in the large parameter space (i.e., viable choices to derive spectrum)

- Normalization:
  - Live time
  - Radiation environment
  - Long-term stability
  - Quality cuts
- Energy dependent:
  - Tracking
  - charge ID
  - electron ID (K-Cut vs BDT)
  - BDT stability (vs efficiency & training)
  - MC model (EPICS vs Geant4)

Systematic uncertainty in electron selection by BDT

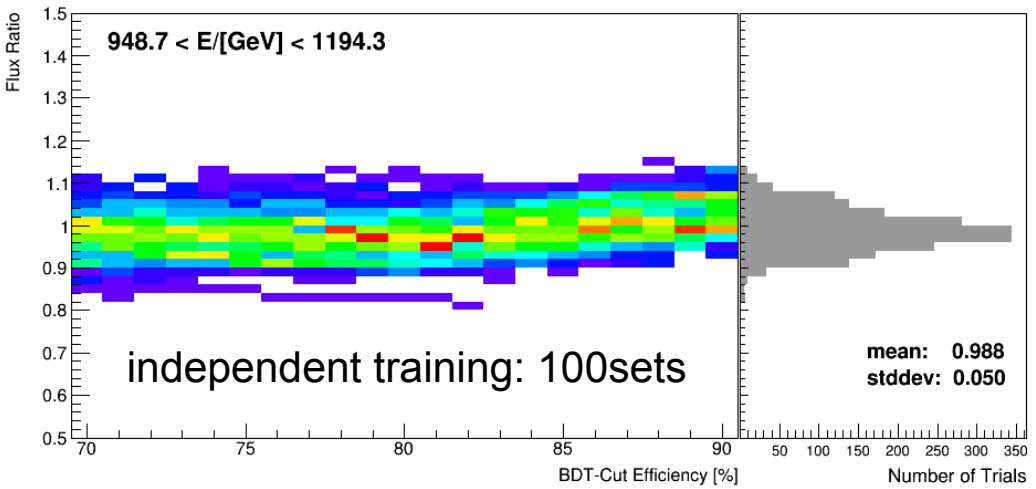

Total systematic uncertainty vs Energy

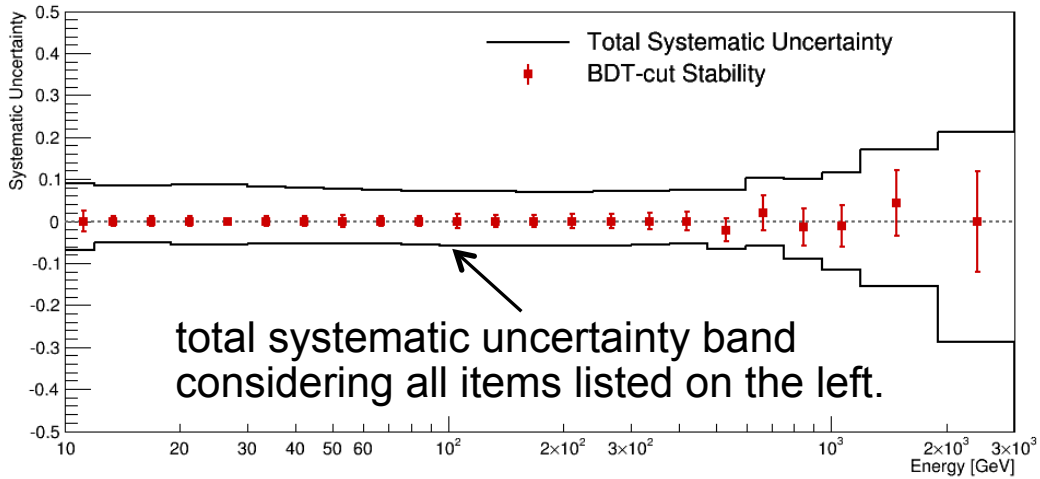

N.B. Energy scale uncertainty is not included in this analysis.

Calibration of Absolute Energy Scale Using Geomagnetic Rigidity Cutoff Energy

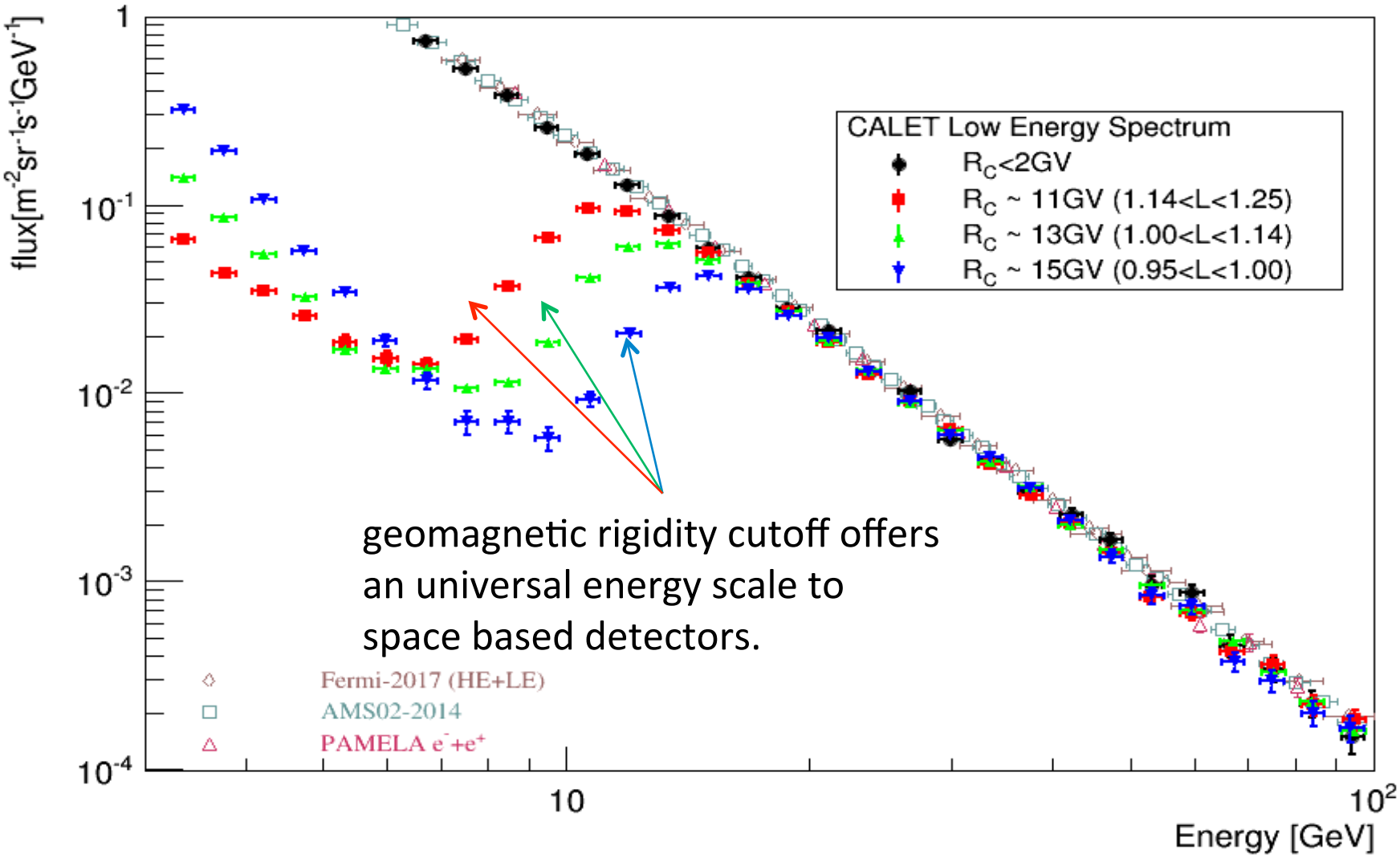

Cutoff Rigidity Measurements and Comparison with Calculation

BEFORE CORRECTION

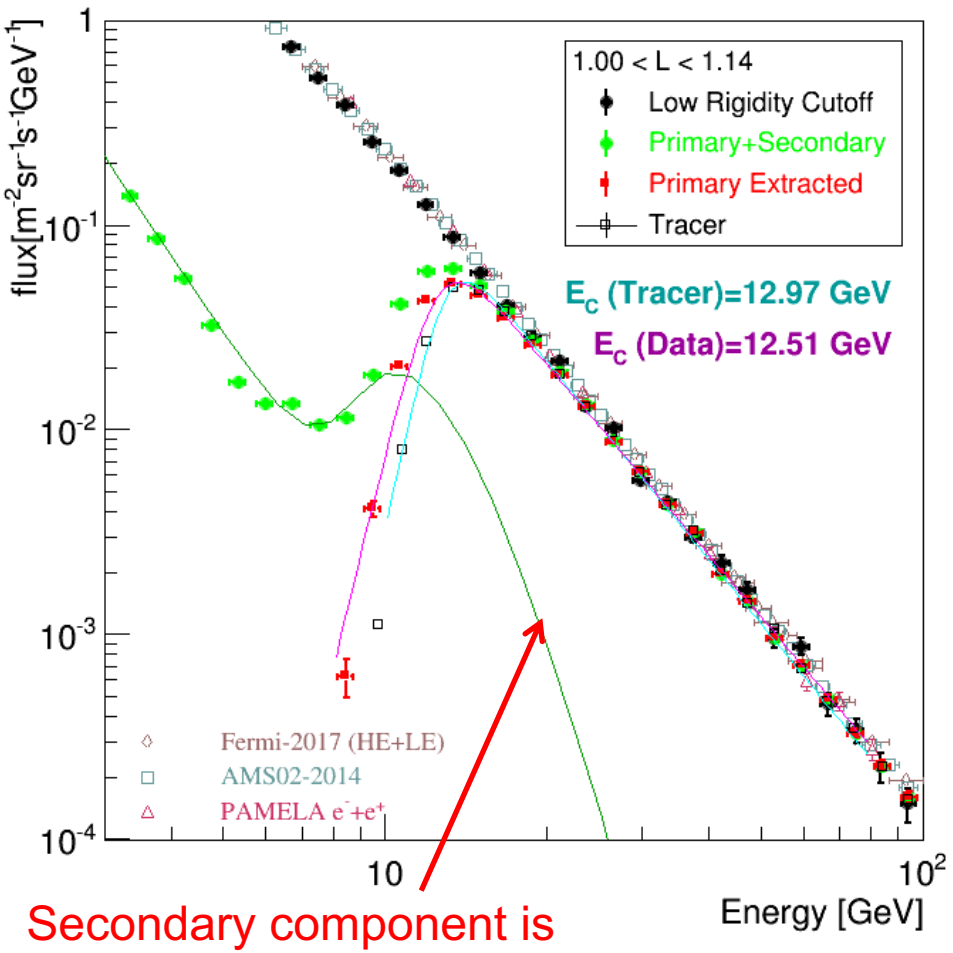

Secondary component is estimated using azimuthal distributions

- Performed in three different cutoff rigidity regions.
- Correction factor was found to be **1.035** compared to MIP calibration.

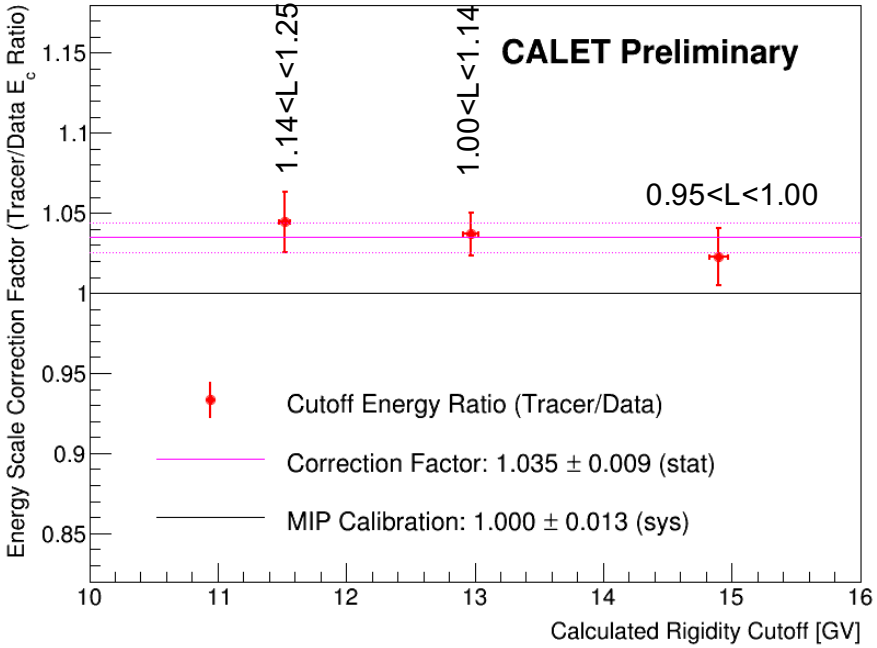

Cutoff Rigidity Measurements and Comparison with Calculation

AFTER CORRECTION

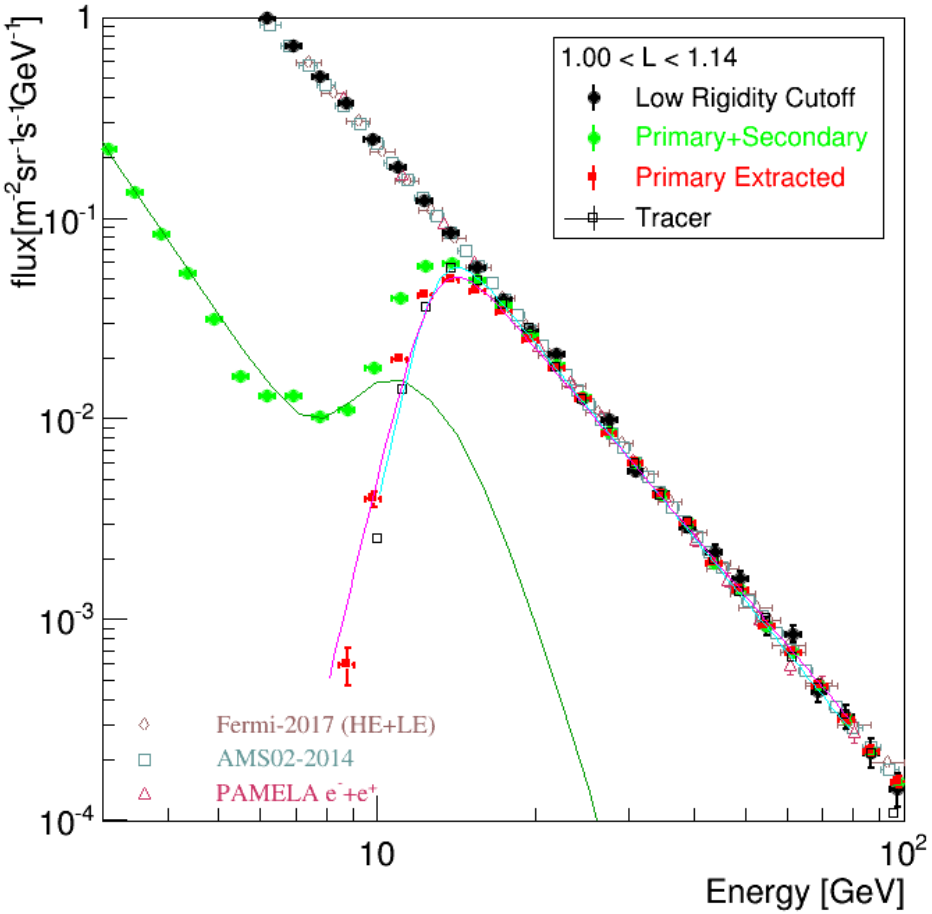

- Performed in three different cutoff rigidity regions.
- Correction factor was found to be **1.035** compared to MIP calibration.

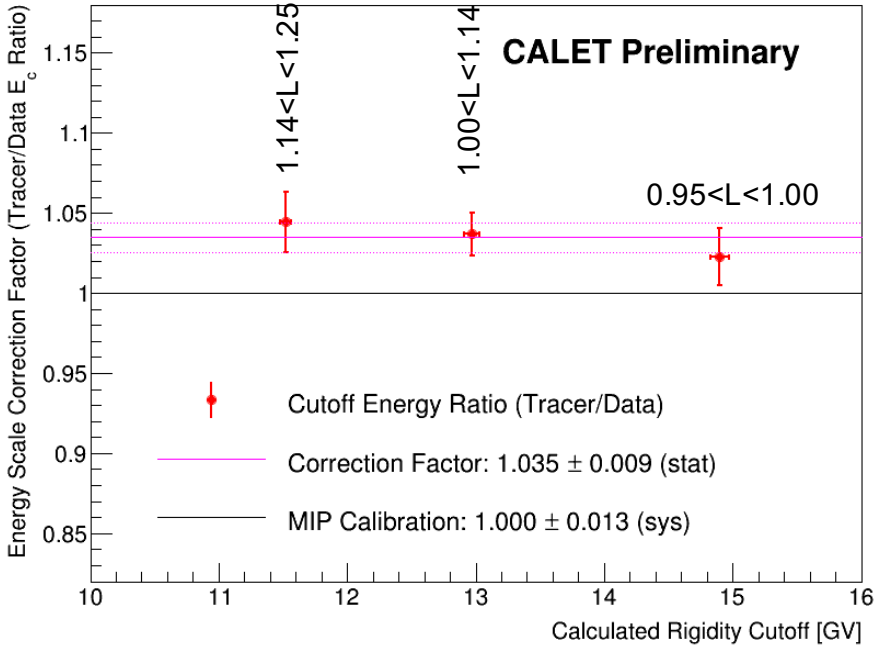

Since universal energy-scale calibration between different instruments is very important, we adopt the energy scale determined by rigidity cutoff to derive our spectrum.

Inclusive (e^++ e^-) Electron Energy Spectrum [10 GeV, ~3TeV]

- Geometry Condition: SΩ= 570.3 cm^2sr (Fully Contained: 55% for all acceptance)
- Live Time: 2015/10/13—2017/06/30 (x 0.85) => T= 4.57 x 10^7 sec
- Exposure: SΩT = 2.64 x 10^6 m^2 sr sec **(less than 20% of full analysis for 5 years)**

Physical Review Letters 119 (2017) 181101, 3 November 2017

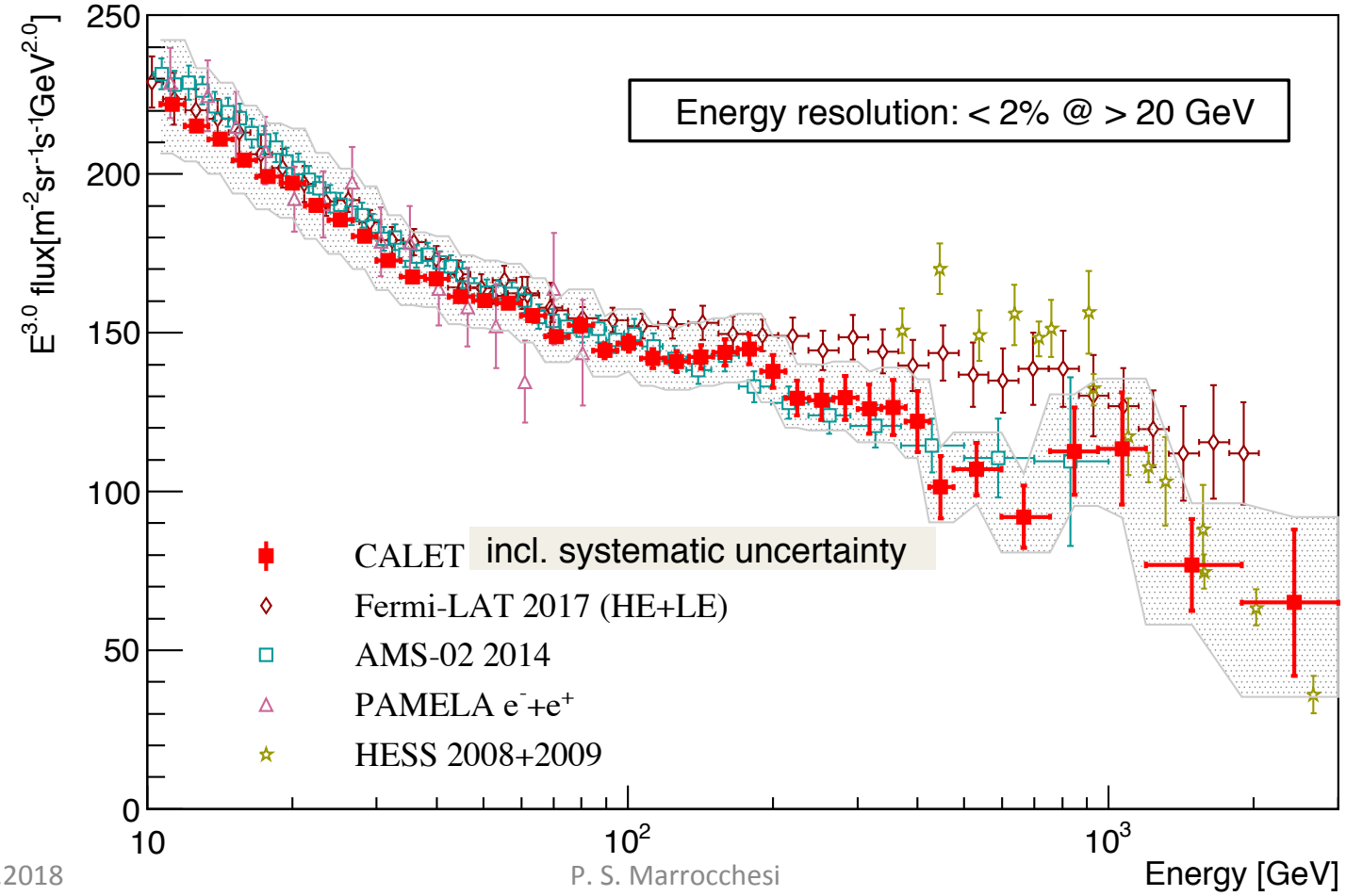

Measurements of the electron spectrum

Comparison of CALET with DAMPE and other experiments in space

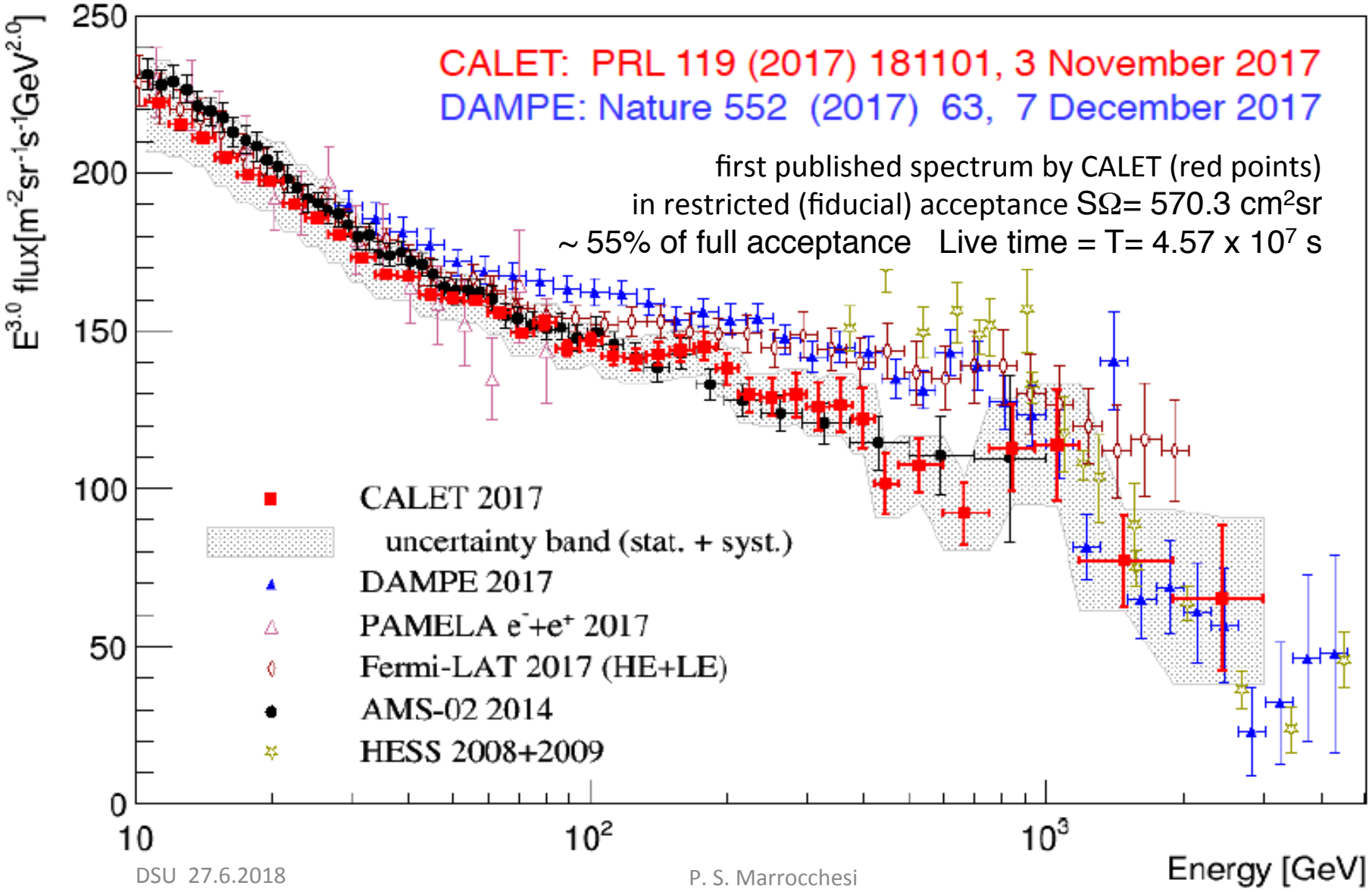

Extended Measurement by CALET

Approximately doubled statistics above 500GeV by using full acceptance of CALET

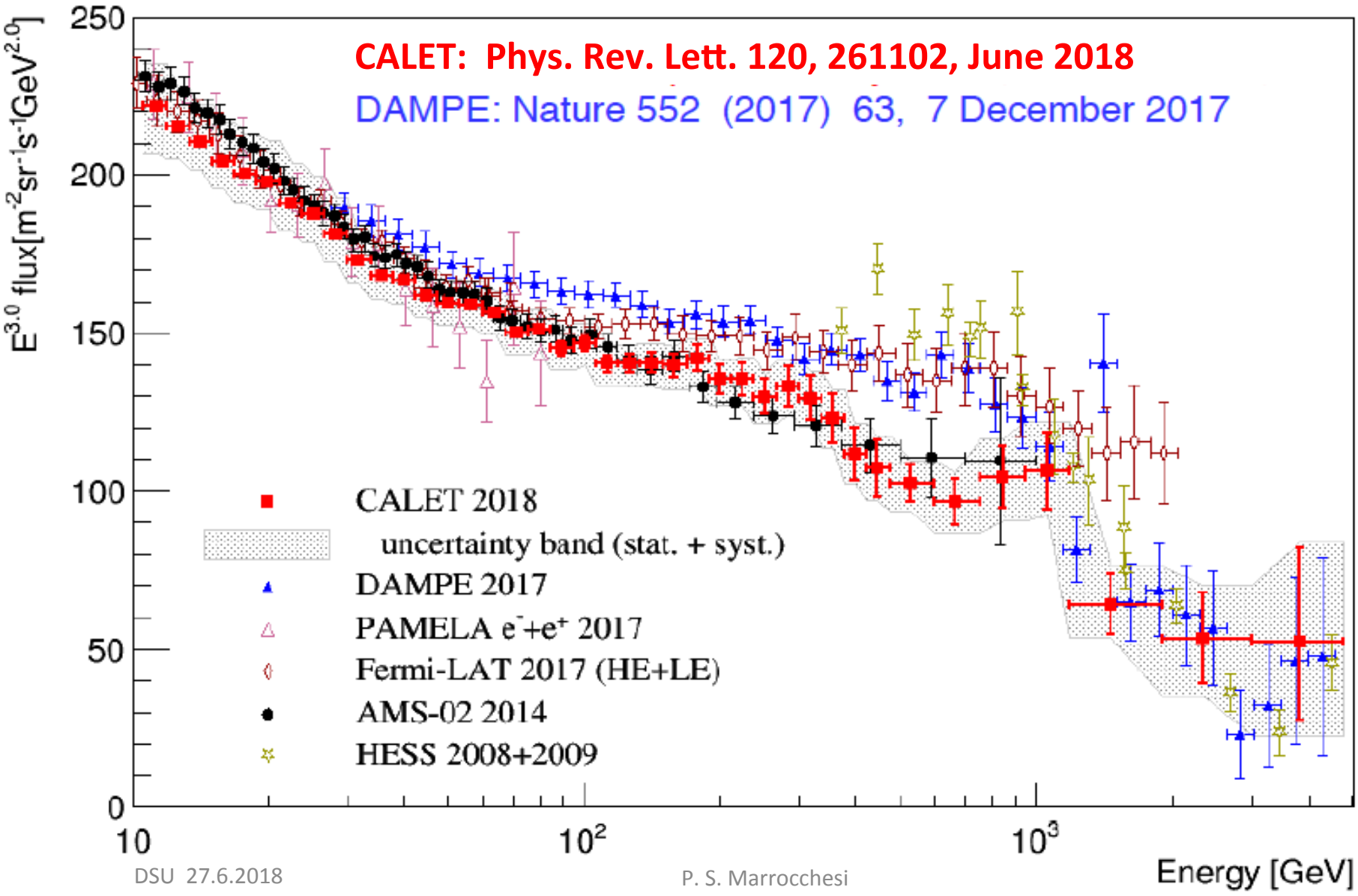

Extended Measurement by CALET

Approximately doubled statistics above 500GeV by using full acceptance of CALET **[11 GeV, 4.8 TeV]**

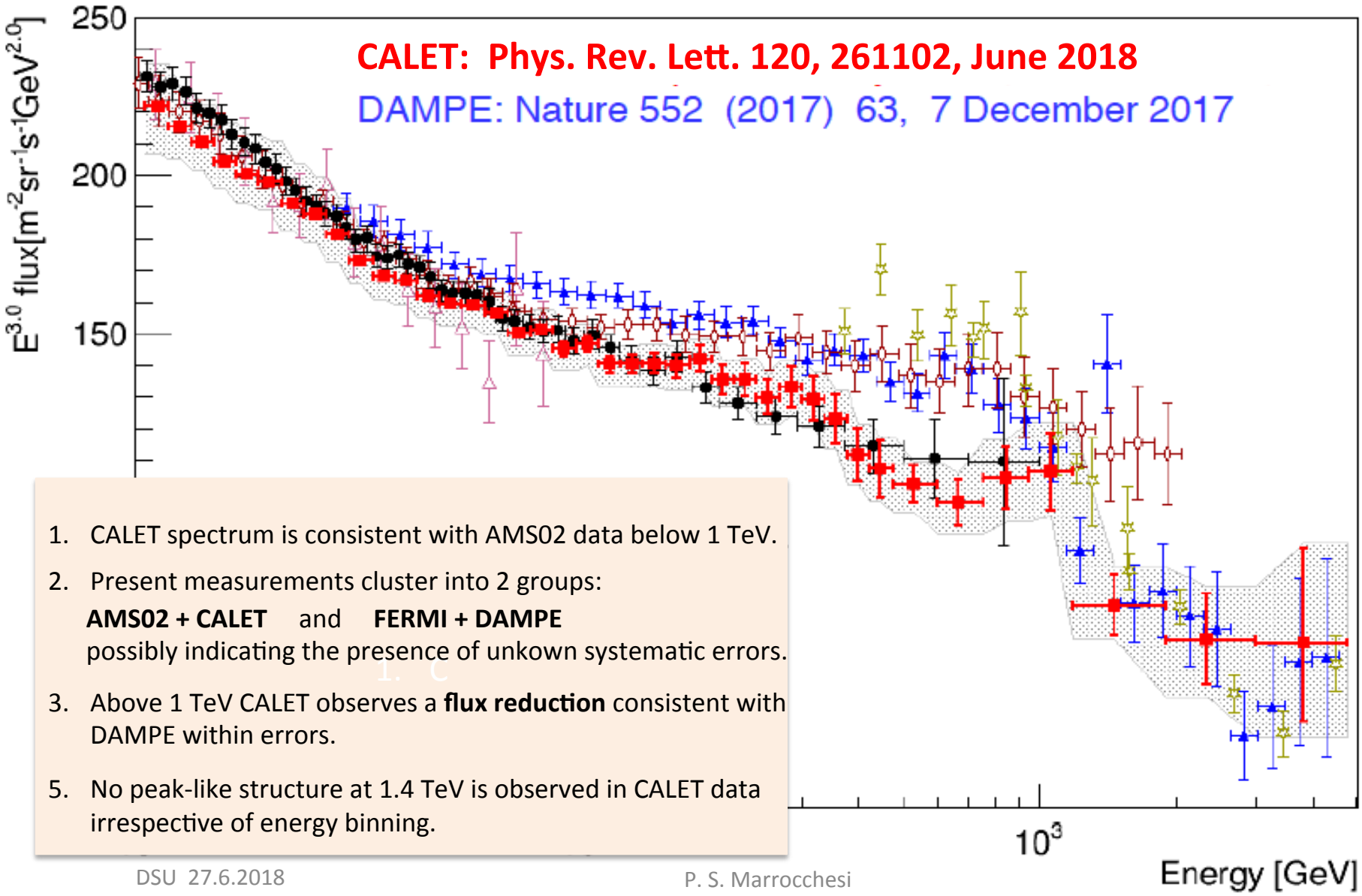

1. CALET spectrum is consistent with AMS02 data below 1 TeV.
2. Present measurements cluster into 2 groups:
   AMS02 + CALET and **FERMI + DAMPE**
   possibly indicating the presence of unkown systematic errors.
3. Above 1 TeV CALET observes a **flux reduction** consistent with DAMPE within errors.
5. No peak-like structure at 1.4 TeV is observed in CALET data irrespective of energy binning.

Comparison of CALET and DAMPE

Is there a peak-like spectral structure at 1.4 TeV ?

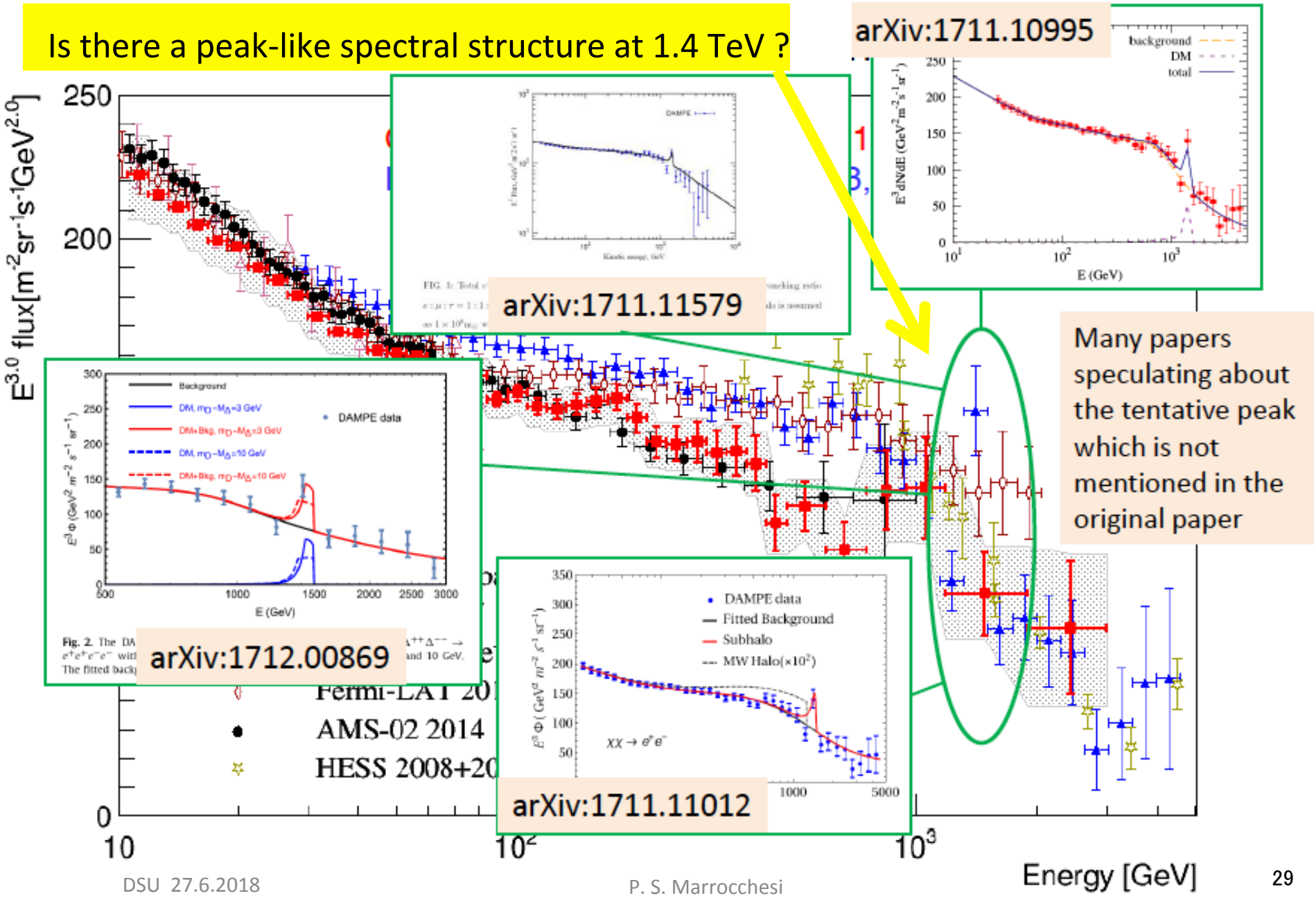

Charge Identification of Nuclei

CHD charge resolution (2 layers combined) vs. Z

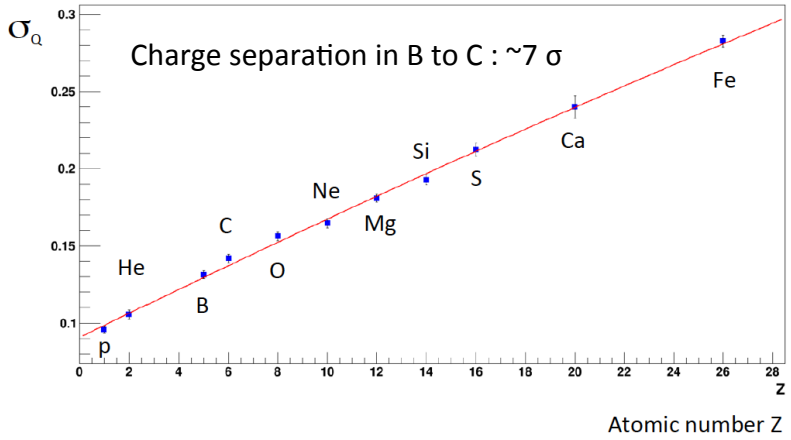

Atomic number Z

Charge resolution using multiple dE/dx measurements from the IMC scintillating fibers.

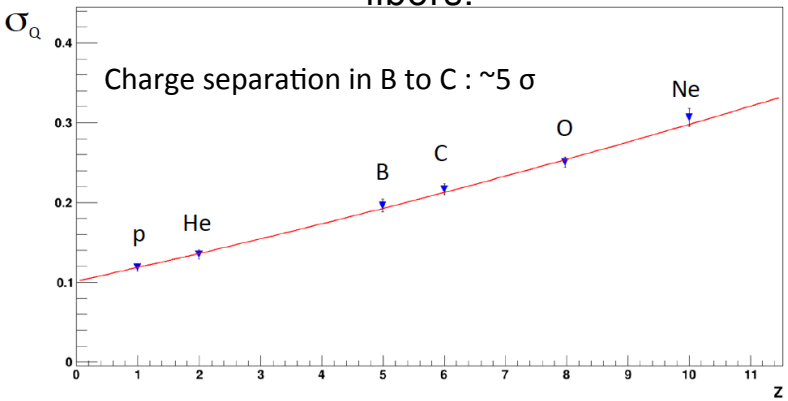

Atomic number Z

Non-linear response to Z^2 is corrected both in CHD and IMC using a model.

Charge resolution combined CHD+IMC

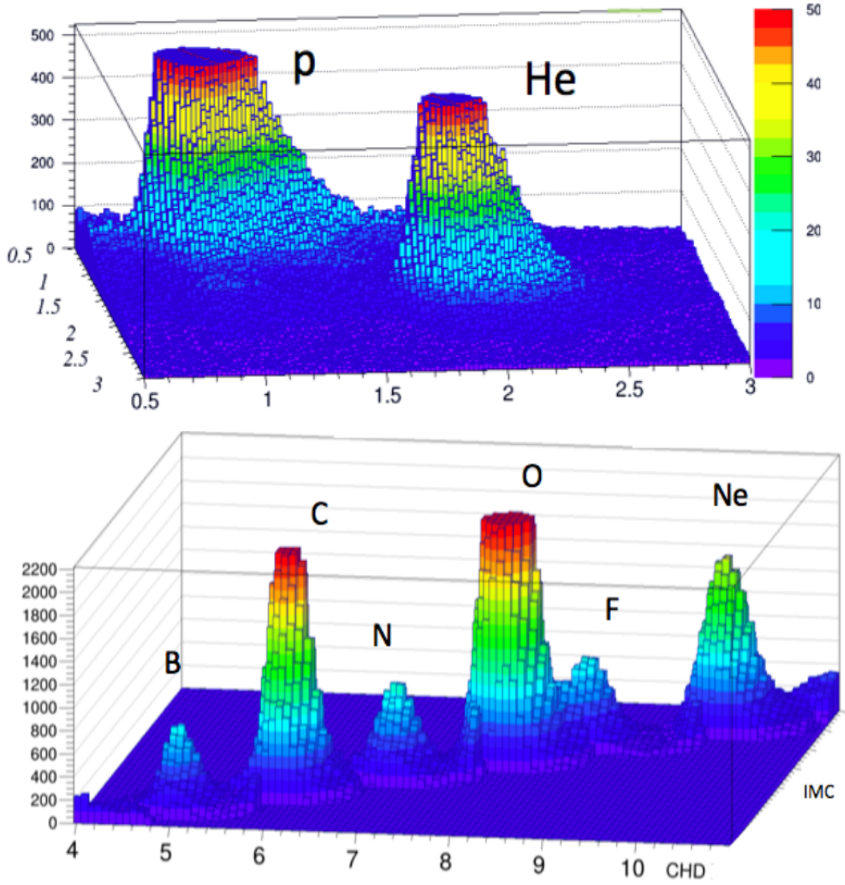

*) Plots are truncated to clearly present the separation.

A clear separation between p, He, ~ Z=8, can be seen from CHD+IMC data analysis.

Preliminary Flux of Primary Components

Flux measurement:

$$\Phi(E) = \frac{N(E)}{S\Omega\varepsilon(E)T\Delta E}$$

N(E): Events in unfolded energy bin
$S\Omega$: Geometrical acceptance
T : Live time
$\varepsilon(E)$: Efficiency
ΔE : Energy bin width

Observation period:
2015.10.13 – 2017.10.31 (750 days)
Selected events: ~13 million

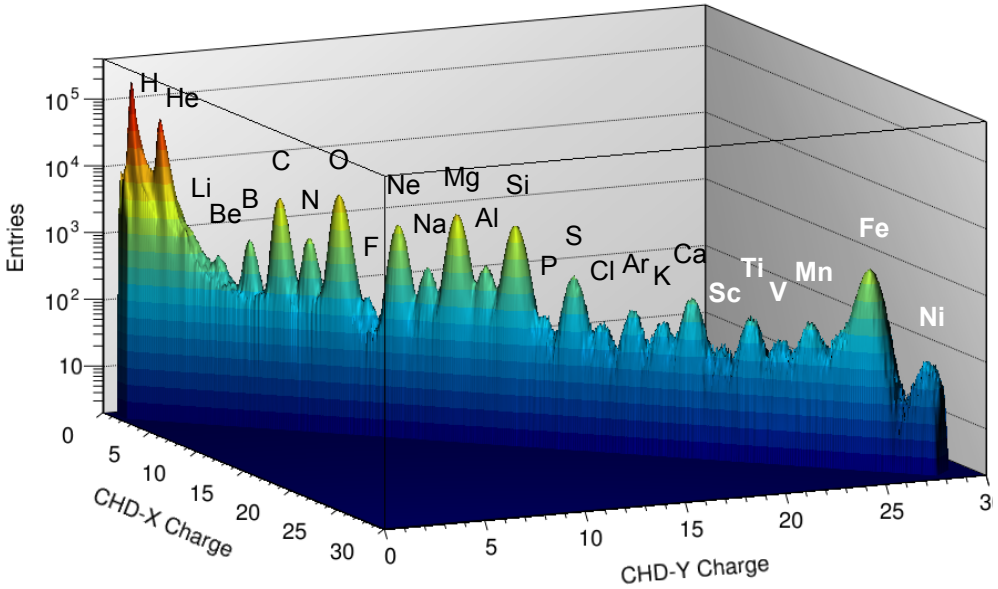

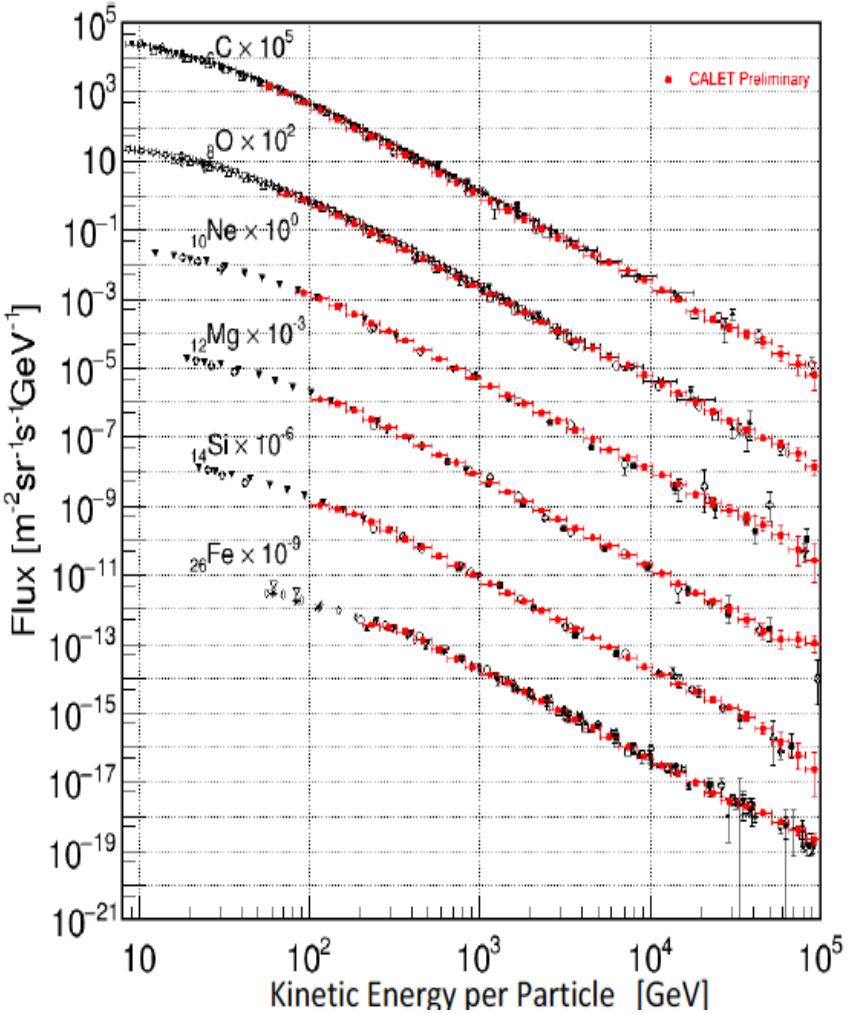

[Y.Akaike]

Preliminary Energy spectra of Carbon and Oxygen (2 independent CALET analyses)

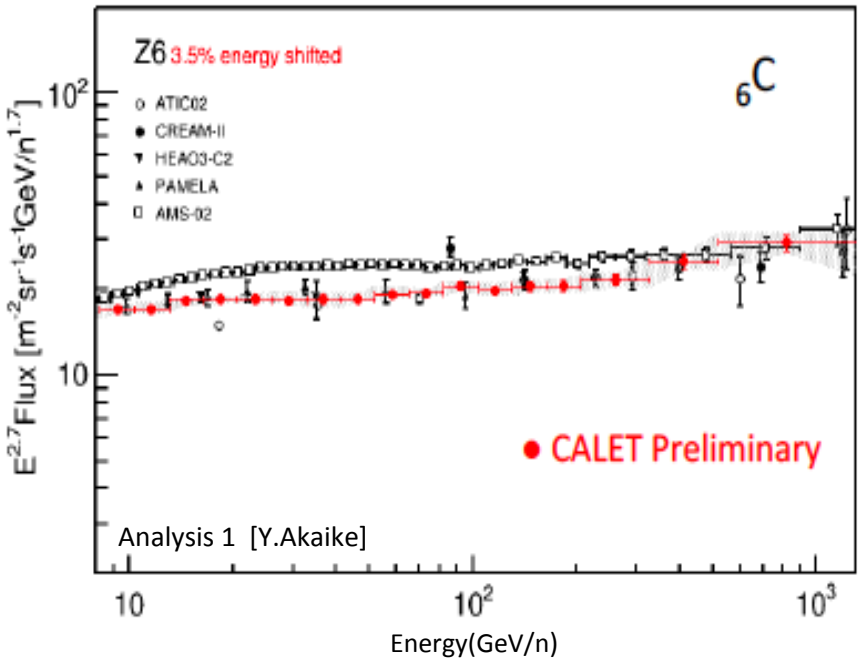

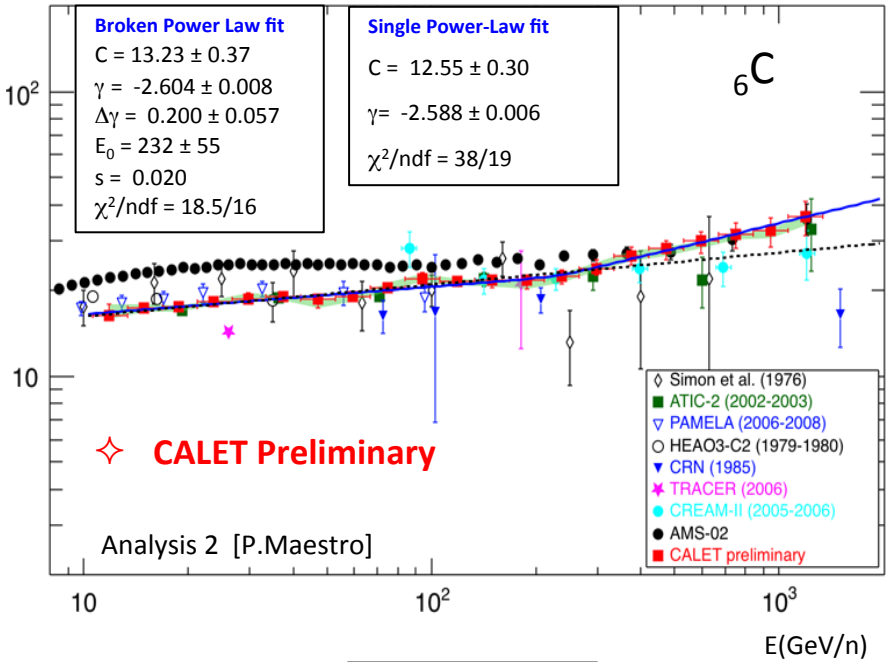

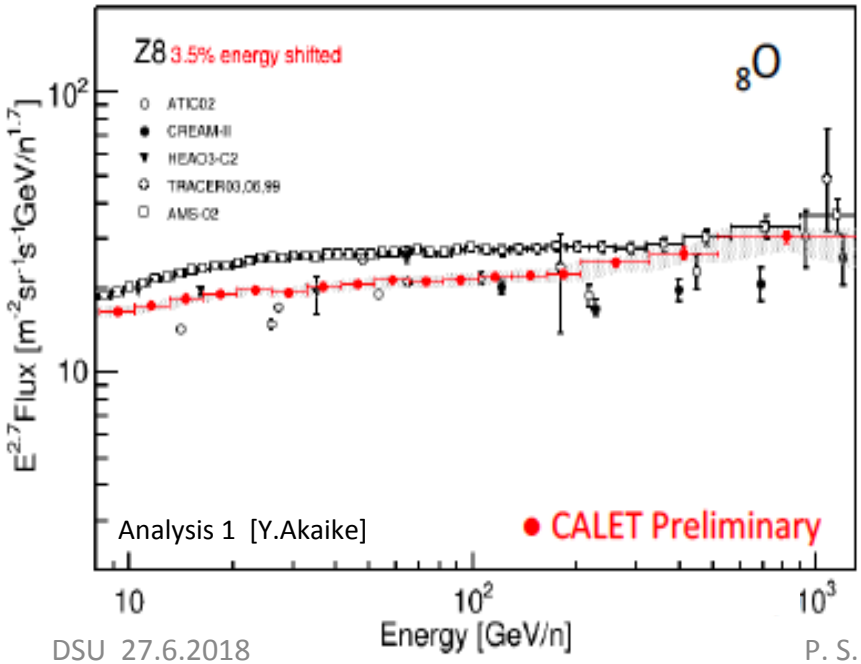

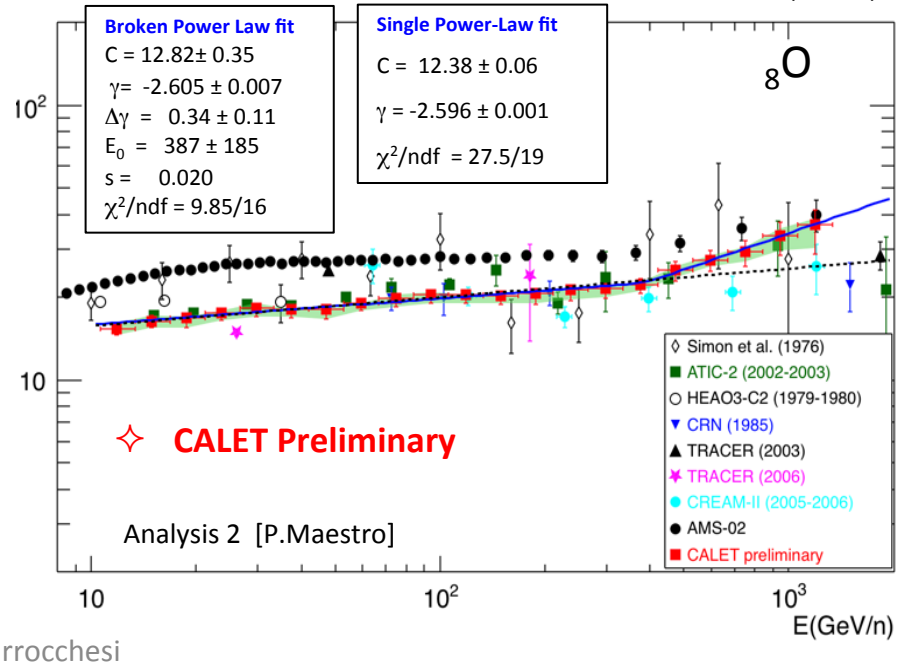

Preliminary Boron-to-Carbon Flux Ratio

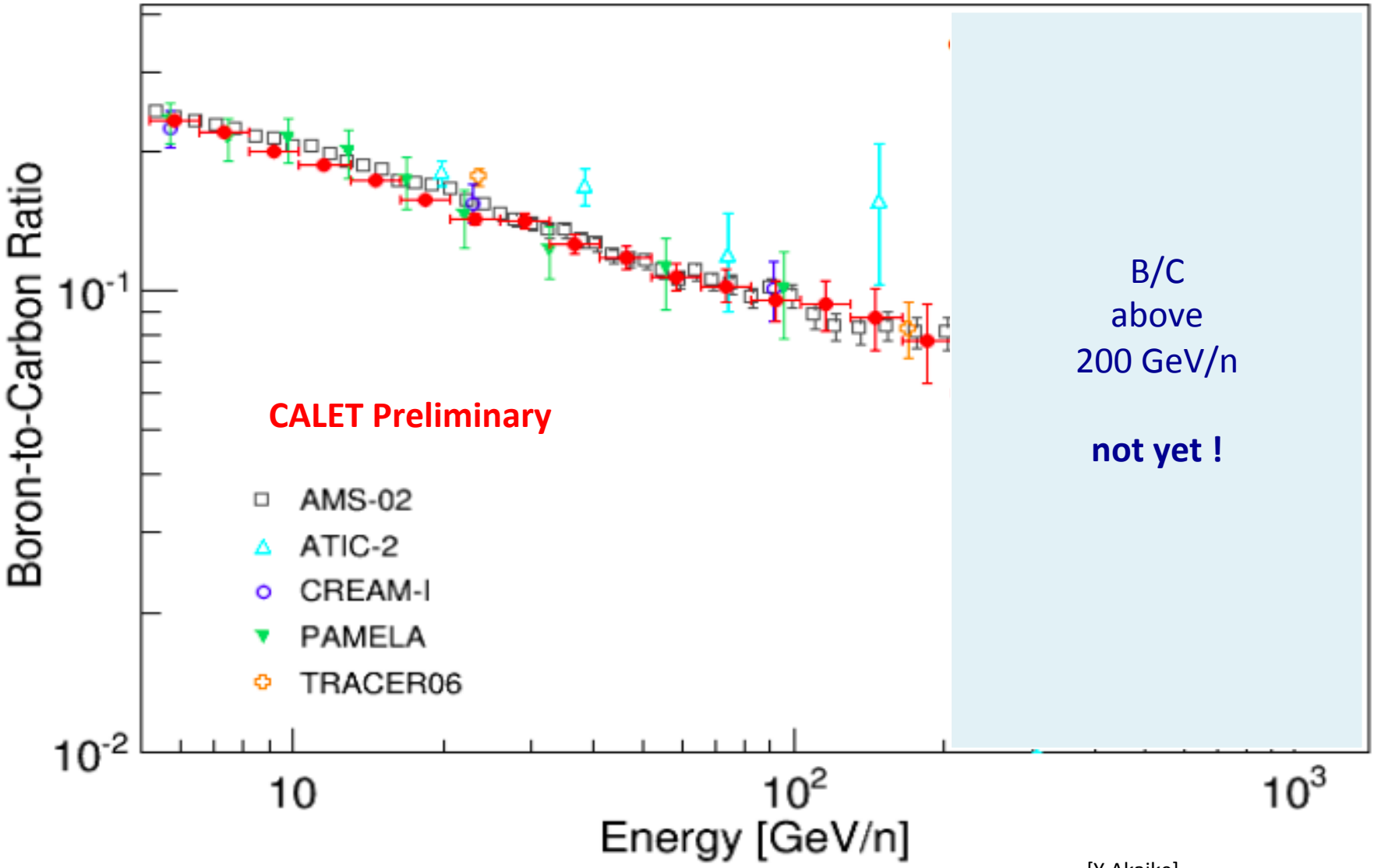

[Y.Akaike]

Preliminary Spectra of Nuclei with **Even** Atomic Number (Z = 10 ÷16)

[Y.Akaike]

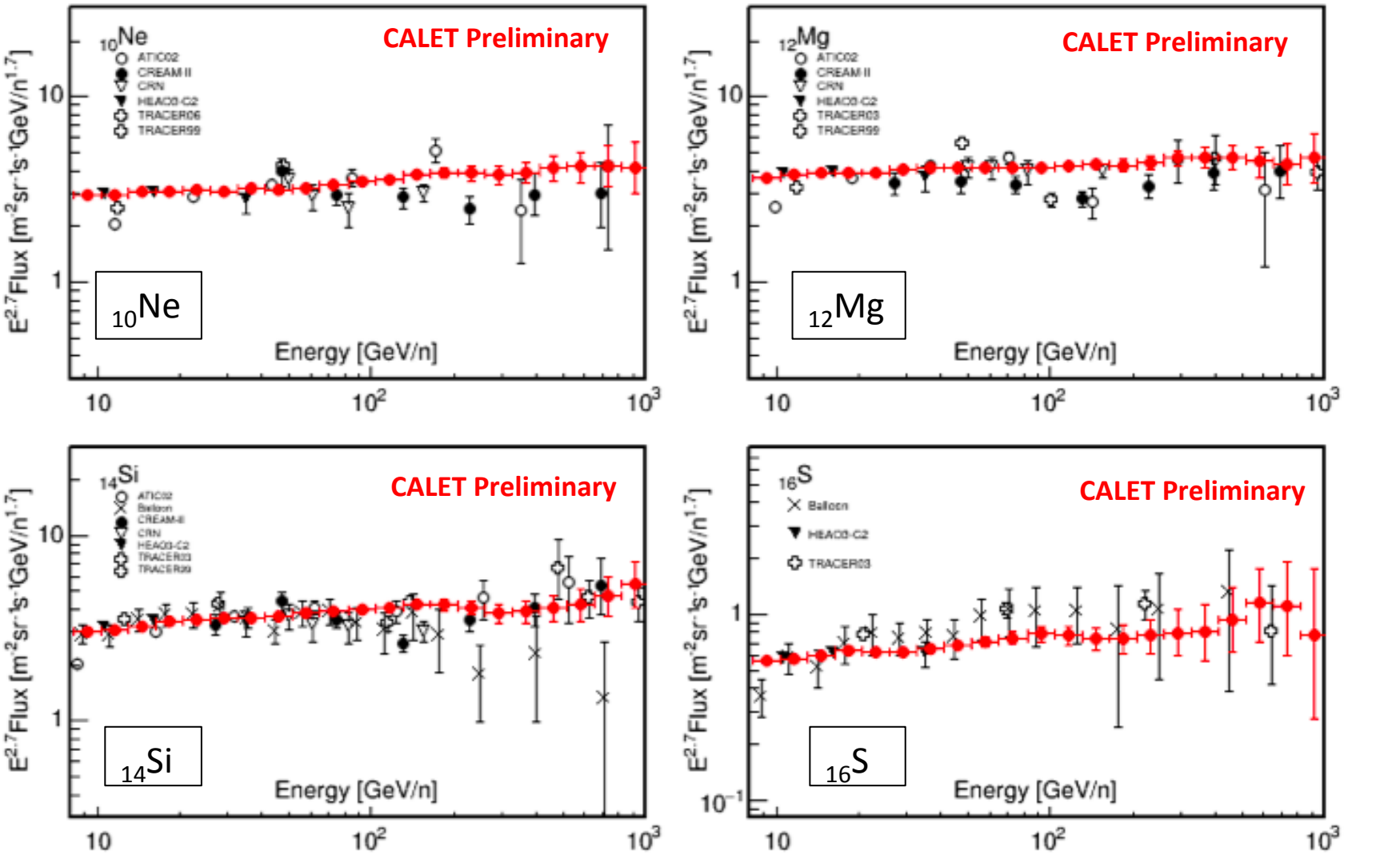

Preliminary Spectra of Nuclei with **Even** Atomic Number (Z = 18 ÷28)

[Y.Akaike]

$_{18}$Ar

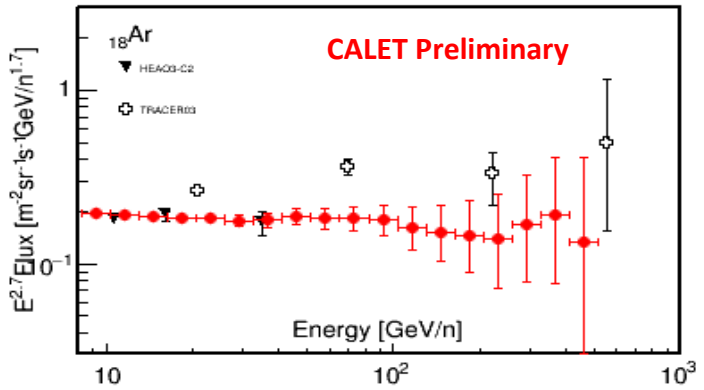

$_{20}$Ca

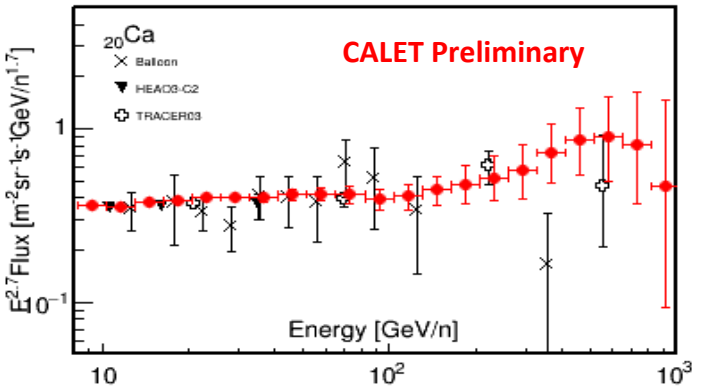

$_{22}$Ti

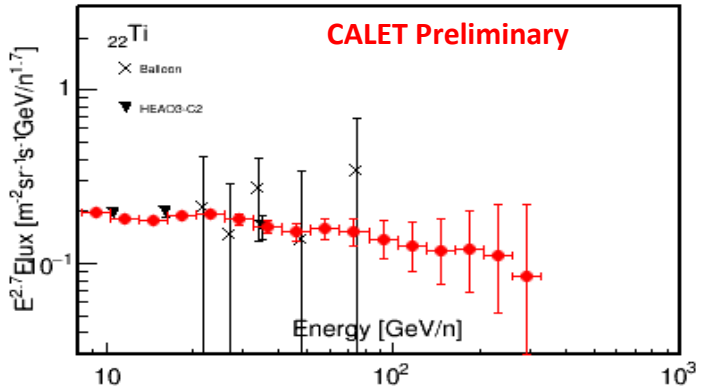

$_{24}$Cr

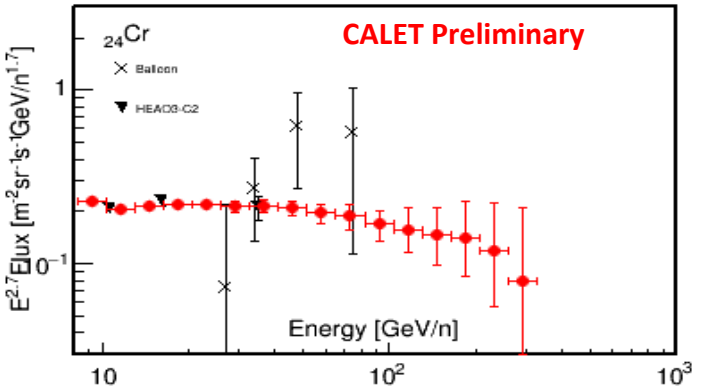

$_{26}$Fe

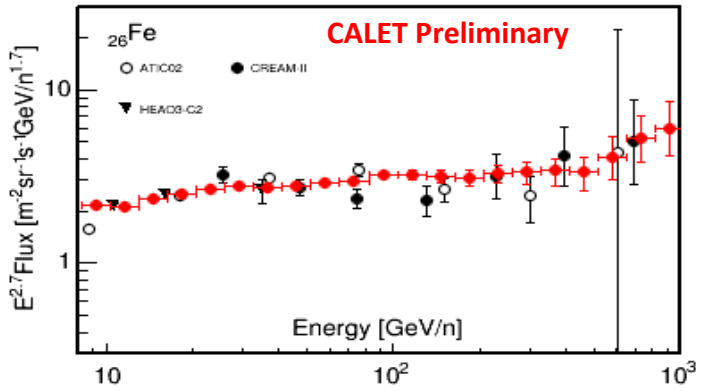

$_{28}$Ni

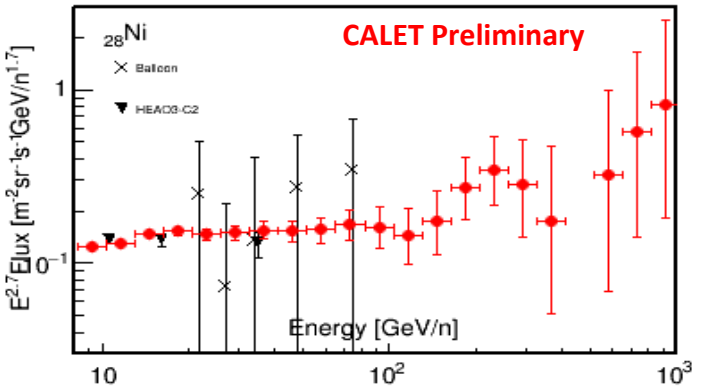

Preliminary Ultra Heavy Nuclei Measurements for $26 < Z \leq 40$

- CALET measures the relative abundances of ultra heavy nuclei through $_{40}$Zr

CALET has a special UH CR trigger utilizing the CHD and the top 4 layers of the IMC that:

- has an expanded geometry factor of ~4000 cm^{2}sr
- has a very high duty cycle due to low event rate

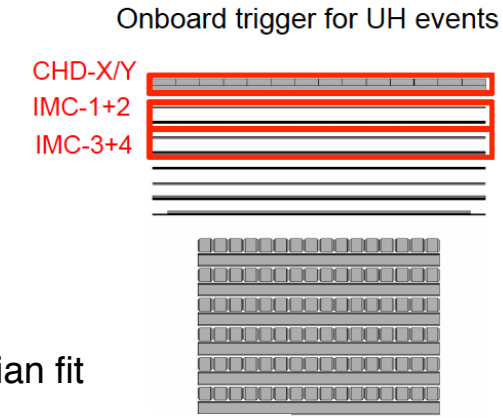

Data analysis

- Event Selection: Vertical cutoff rigidity > 4GV & Zenith Angle < 60 degrees
- Contamination from neighboring charge are determined by multiple-Gaussian fit

Charge distribution

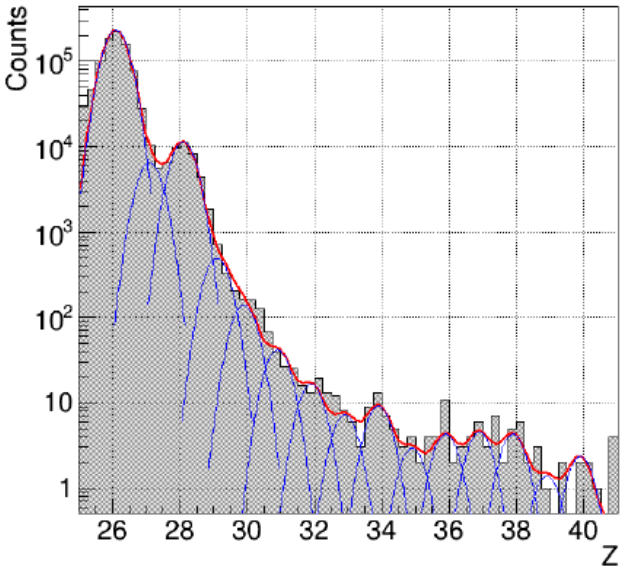

Relative abundance (Fe=1)

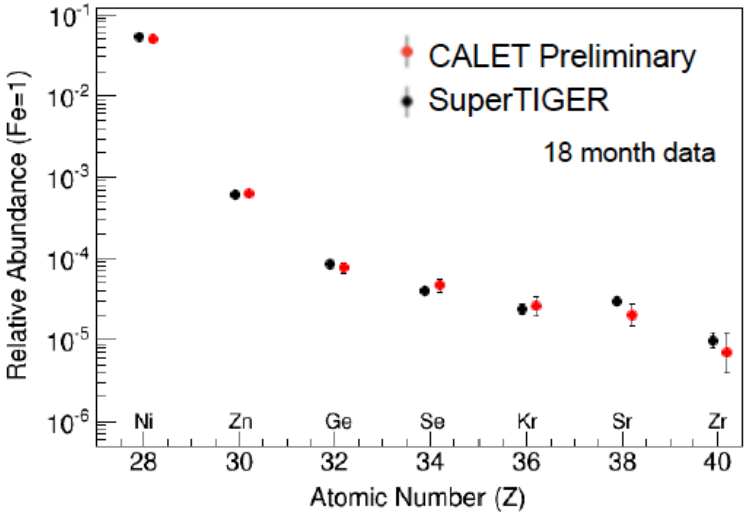

CALET γ–ray Sky in LE (>1GeV) Trigger

Exposure map

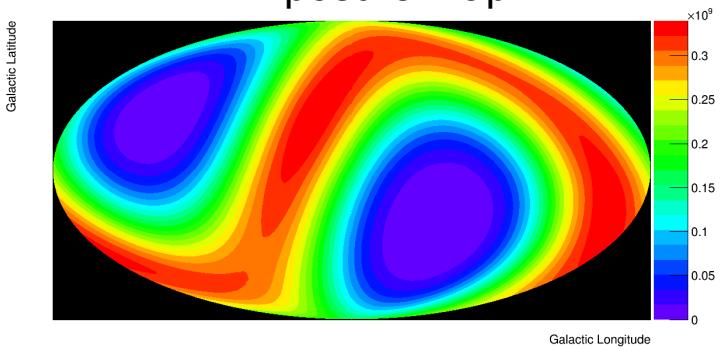

Exposure is limited to low latitude regions
=> |declination| > 60 deg is hardly seen
in LE gamma-ray trigger mode.
2015/11 – 2016/05

151101-180131 E>1GeV Gamma-ray sky map

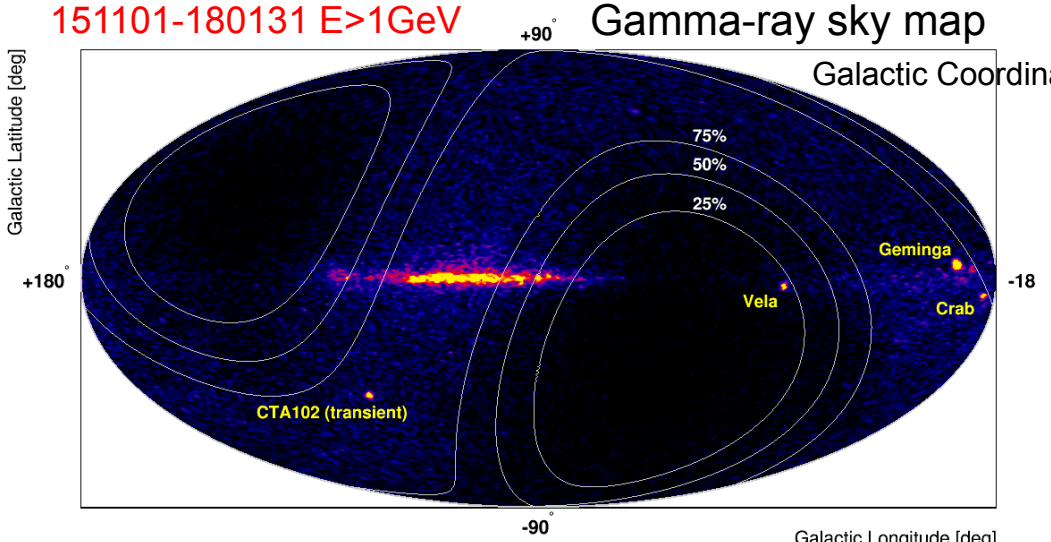

Geminga:432 Vela:138 Crab:150 All: 45740

Galactic diffuse gamma-rays

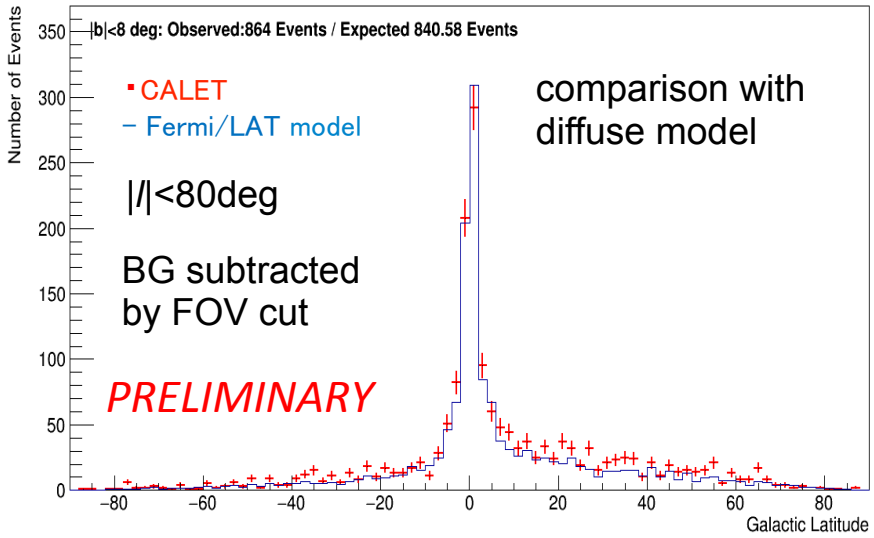

Gamma-ray energy spectrum

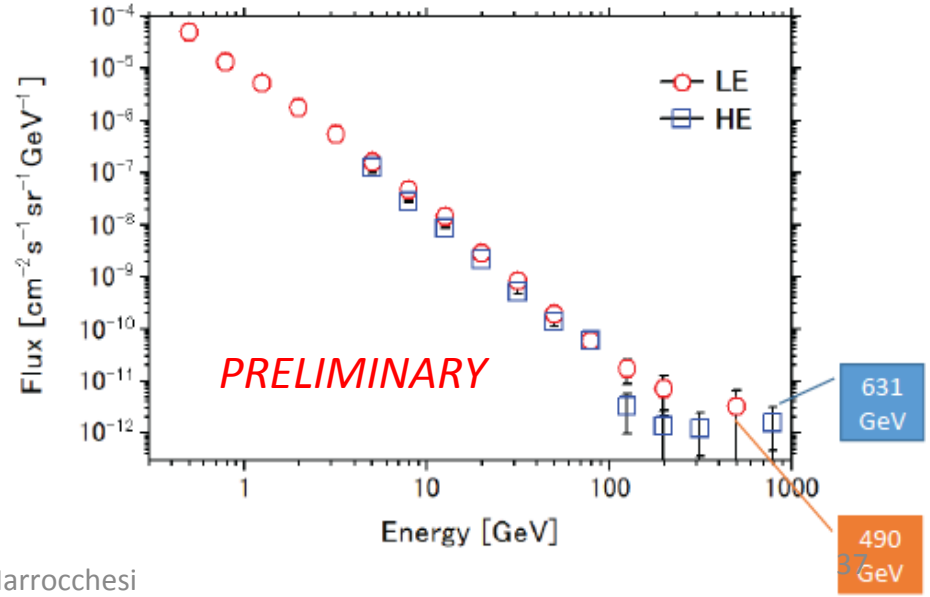

CALET Gamma-ray Burst Monitor (CGBM)

Hard X-ray Monitor (HXM)

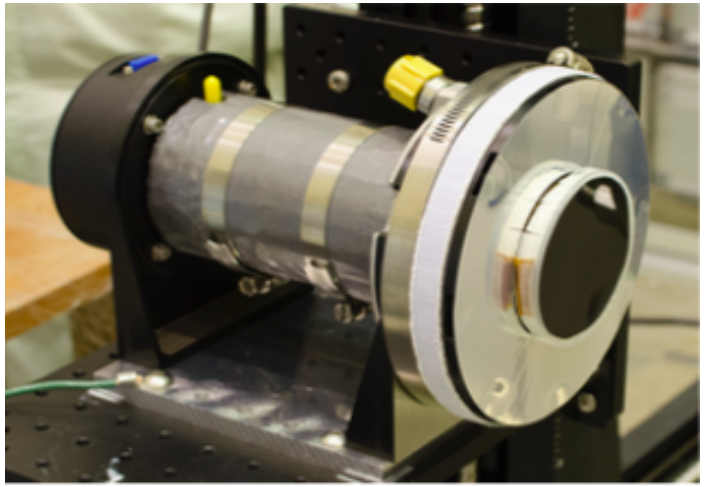

Soft Gamma-ray Monitor (SGM)

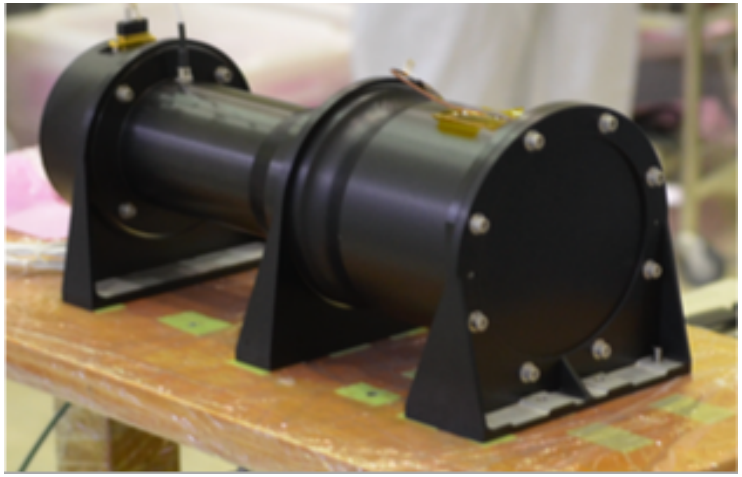

	HXM (x2)	SGM
Detector (Crystal)	$LaBr_3(Ce)$	BGO
Number of detector	2	1
Diameter [mm]	61	102
Thickness [mm]	12.7	76
Energy range [keV]	7-1000	100-20000
Energy resolution@662 keV	~3%	~15%
Field of view	~3 sr	~2π sr

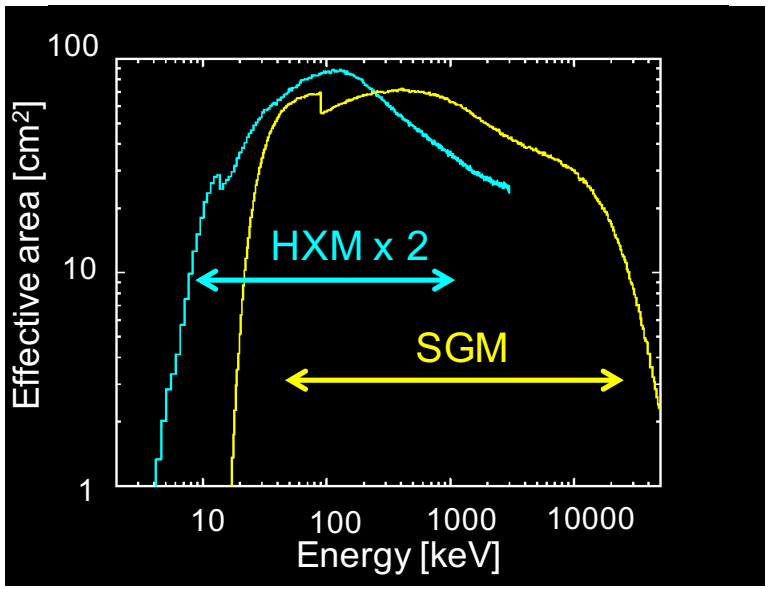

Summary of gamma-ray burst observations

CGBM Operation Status

- Scientific observation: October 6, 2015
- Observation efficiency: ~60% (HV-on time)
- On-board trigger alert (GCN notice)
  (http://gcn.gsfc.nasa.gov/calet_triggers.html)

CGBM GRB Statistics

(As of Sep 30, 2017)

- 74 GRBs (only confirmed GRBs)
- GRB rate: ~37 GRBs/yr
- 63 long GRBs (85%), 11 short GRBs (15%)

c.f., Fermi-GBM: 82% long GRBs, 18% short GRBs (Paciesas et al. 2012)

- 49 spectroscopic GRB samples

CALET UPPER LIMITS ON X-RAY AND GAMMA-RAY COUNTERPARTS OF GW 151226

Astrophysical Journal Letters 829:L20(5pp), 2016 September 20

The CGBM covered 32.5% and 49.1% of the GW 151226 sky localization probability in the 7 keV - 1 MeV and 40 keV - 20 MeV bands respectively. We place a 90% upper limit of 2×10^{-7} erg cm^{-2} s^{-1} in the 1 - 100 GeV band where CAL reaches 15% of the integrated LIGO probability (~1.1 sr). The CGBM 7 σ upper limits are 1.0×10^{-6} erg cm^{-2} s^{-1} (7-500 keV) and 1.8×10^{-6} erg cm^{-2} s^{-1} (50-1000 keV) for one second exposure. Those upper limits correspond to the luminosity of 3-5 $\times 10^{49}$ erg s^{-1} which is significantly lower than typical short GRBs.

CGBM light curve at the moment of the GW151226 event

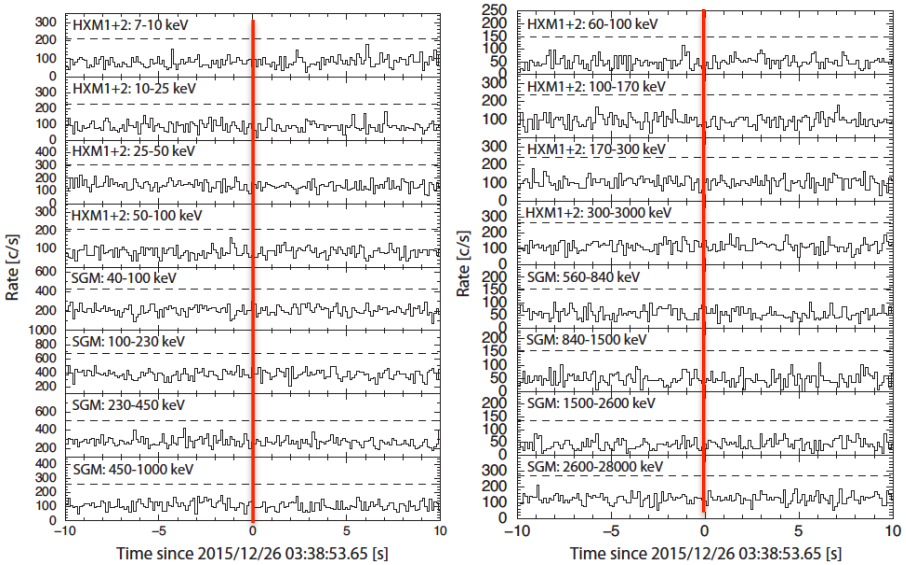

Figure 1. The CGBM light curves in 0.125 s time resolution for the high-gain data (left) and the low-gain data (right). The time is offset from the LIGO trigger time of GW 151226. The dashed-lines correspond to the 5 σ level from the mean count rate using the data of ±10 s.

Upper limit for gamma-ray burst monitors and Calorimeter

HXM: 7-500 keV

SGM: 50-1000 keV

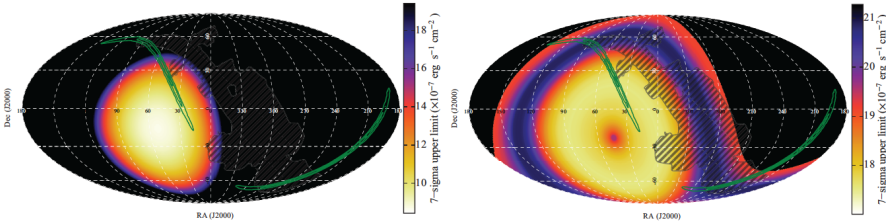

Figure 2. The sky maps of the 7 σ upper limit for HXM (left) and SGM (right). The assumed spectrum for estimating th upper limit is a typical BATSE S-GRBs (see text for details). The energy bands are 7-500 keV for HXM and 50-1000 keV fo SGM. The GW 151226 probability map is shown in green contours. The shadow of ISS is shown in black hatches.

Calorimeter: 1-100 GeV

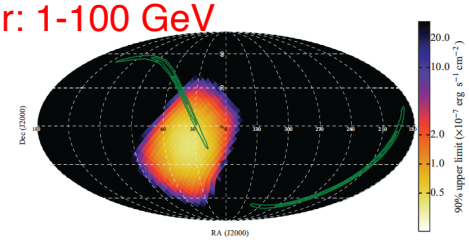

Figure 3. The sky map of the 90% upper limit for CAL in the 1-100 GeV band. A power-law model with a photon index of −1 is used to calculate the upper limit. The GW 151226 probability map is shown in green contours.

CALET's first publication was NOT for Cosmic Rays

Accepted article online 25 APR 2016

Geophysical Research Letters

Relativistic electron precipitation at International Space Station: Space weather monitoring by Calorimetric Electron Telescope

Ryuho Kataoka[1,2], Yoichi Asaoka[3], Shoji Torii[3,4], Toshio Terasawa[5], Shunsuke Ozawa[4], Tadahisa Tamura[6], Yuki Shimizu[6], Yosui Akaike[4], and Masaki Mori[7]

[1]Space and Upper Atmospheric Sciences Group, National Institute of Polar Research, Tachikawa, Japan, [2]Department of Polar Science, School of Multidisciplinary Sciences, SOKENDAI (Graduate University for Advanced Studies), Tachikawa, Japan, [3]Research Institute for Science and Engineering, Waseda University, Shinjuku, Japan, [4]Department of Physics, Waseda University, Shinjuku, Japan, [5]Institute for Cosmic Ray Research, University of Tokyo, Kashiwa, Japan, [6]Institute of Physics, Kanagawa University, Yokohama, Japan, [7]Department of Physical Sciences, Ritsumeikan University, Kusatsu, Japan

Abstract The charge detector (CHD) of the Calorimetric Electron Telescope (CALET) on board the International Space Station (ISS) has a huge geometric factor for detecting MeV electrons and is sensitive to relativistic electron precipitation (REP) events. During the first 4 months, CALET CHD observed REP events mainly at the dusk to midnight sector near the plasmapause, where the trapped radiation belt electrons can be efficiently scattered by electromagnetic ion cyclotron (EMIC) waves. Here we show that interesting 5–20 s periodicity regularly exists during the REP events at ISS, which is useful to diagnose the wave-particle interactions associated with the nonlinear wave growth of EMIC-triggered emissions.

Space Weather is now a new topic of CALET observations !

Relativistic Electron Precipitation

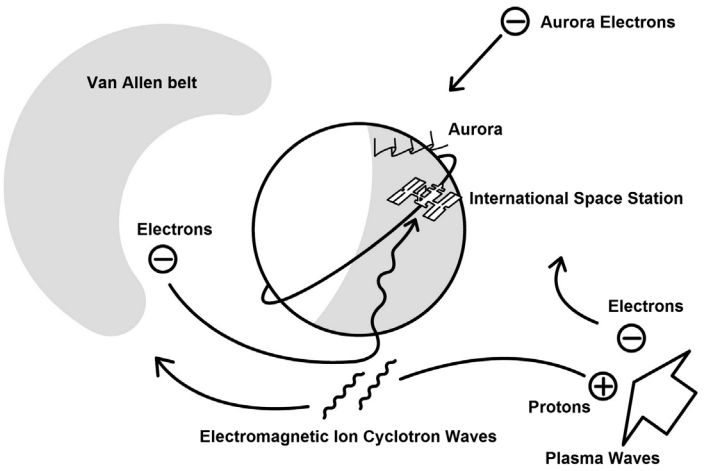

CHD X and Y count rate increase by REP

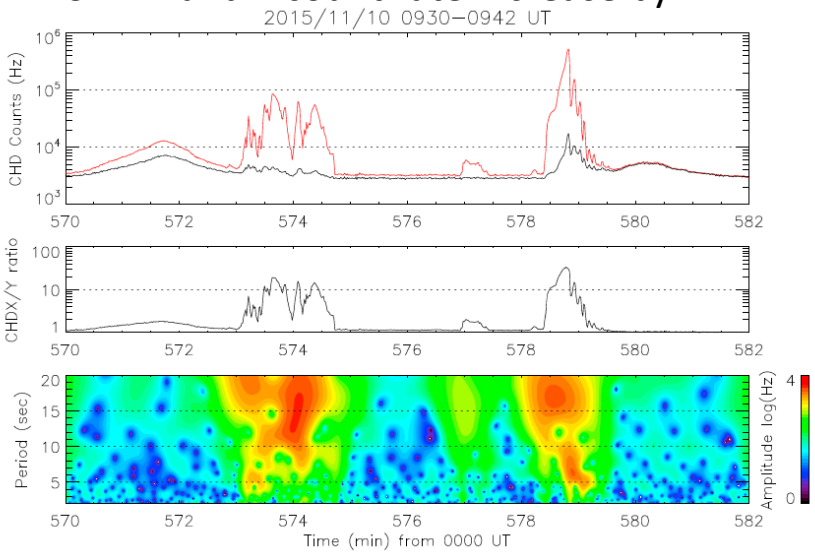

Summary and Future Prospects

- CALET was successfully launched on Aug. 19th, 2015. The observation campaign started on Oct. 13th, 2015. Excellent performance and remarkable stability of the instrument.
- As of Feb. 28, 2018, total observation time is 870 days with live time fraction to total time close to 85 %. Nearly 570 million events collected with high energy (>10 GeV) trigger.
- Accurate calibrations have been performed with non-interacting p & He events + linearity in the energy measurements established up to 10^6 MIP.
- Preliminary analysis of nuclei, electrons (+ positrons) and gamma-rays have successfully been carried out and spectra obtained in the energy range:
  proton: 50 GeV~100 TeV, helium: 10 GeV-20 TeV/n, C-Fe: 300 GeV~100 TeV,
  B/C ratio: 20 GeV/n-1TeV/n, All electrons: 10 GeV~4.5 TeV.
- Preliminary analysis of UH cosmic rays up to Z=40.
- CALET's CGBM detected 74 GRBs in the energy range 7 keV-20 MeV. Follow-up observations of the GW events were carried out.
- The so far excellent performance of CALET and the outstanding quality of the data suggest that a 5-year observation period is likely to provide a wealth of new interesting results.

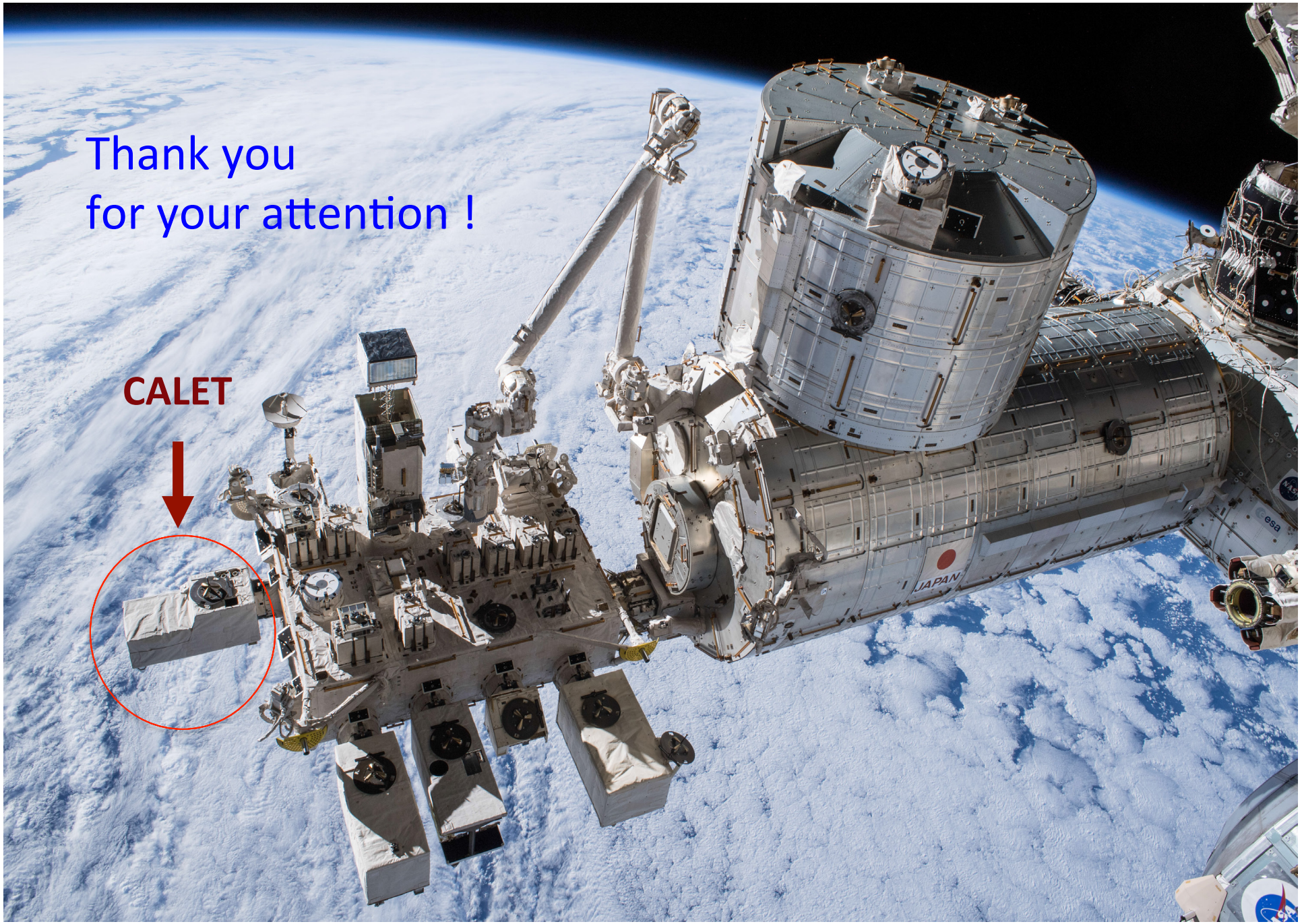
Thank you
for your attention !
CALET
JAPAN